

UWL REPOSITORY
repository.uwl.ac.uk

Combined non-destructive testing (NDT) method for the evaluation of the mechanical characteristics of ultra high performance fibre reinforced concrete (UHPFRC)

Tsioulou, Ourania, Lampropoulos, Andreas and Paschalis, Spyridon (2017) Combined non-destructive testing (NDT) method for the evaluation of the mechanical characteristics of ultra high performance fibre reinforced concrete (UHPFRC). *Construction and Building Materials*, 131. pp. 66-77. ISSN 0950-0618

<http://dx.doi.org/10.1016/j.conbuildmat.2016.11.068>

This is the Accepted Version of the final output.

UWL repository link: <https://repository.uwl.ac.uk/id/eprint/8159/>

Alternative formats: If you require this document in an alternative format, please contact: open.research@uwl.ac.uk

Copyright: Creative Commons: Attribution-Noncommercial-No Derivative Works 4.0

Copyright and moral rights for the publications made accessible in the public portal are retained by the authors and/or other copyright owners and it is a condition of accessing publications that users recognise and abide by the legal requirements associated with these rights.

Take down policy: If you believe that this document breaches copyright, please contact us at open.research@uwl.ac.uk providing details, and we will remove access to the work immediately and investigate your claim.

Rights Retention Statement:

1 Combined Non-Destructive Testing (NDT) method for the evaluation of the 2 mechanical characteristics of Ultra High Performance Fibre Reinforced 3 Concrete (UHPFRC)

4 Ourania Tsioulou, Andreas Lampropoulos* and Spyridon Paschalis
5 School of Environment and Technology, University of Brighton, Lewes Road, Brighton, BN2 4GJ,
6 UK

7 *Corresponding author, email: a.lampropoulos@brighton.ac.uk

8 ABSTRACT

9 Ultra-High Performance Fibre Reinforced Concrete is a material which is becoming increasingly
10 popular in structural applications, mainly due to its superior mechanical characteristics. The
11 mechanical properties of this material are of high importance and the development of non-destructive
12 techniques is vital for the evaluation of the mechanical characteristics of existing structures. In the
13 current study, Ultra-High Performance Fibre Reinforced Concrete with different amounts of steel
14 fibres has been examined. Compressive and tensile tests have been conducted alongside with
15 Ultrasonic Pulse Velocity and Rebound Hammer measurements and the development of appropriate
16 empirical non-destructive models has been examined.

17 *Keywords:* UHPFRC, NDT, Rebound Hammer, Ultrasonic, SonReb,

18 1. Introduction

19 Ultra High Performance Fibre Reinforced Concrete (UHPFRC) is a novel material with superior
20 strength and energy absorption [1]. UHPFRC composition differs to that of an ordinary concrete as it
21 contains low water over cement ratio, silica fume, steel fibres and silica sand. Steel fibres content is
22 one of the most crucial parameters of the mix and important mechanical characteristics such as the
23 tensile strength, the flexural strength and the ductility of UHPFRC elements are highly affected by the
24 percentage of steel fibres. According to previously published studies [2-7], increment of steel fibres
25 amount results to an increment of the flexural strength. In literature [1, 8-11], there are several
26 investigations on the mechanical properties of UHPFRC based on conventional destructive methods.
27 However, there are very limited studies on the evaluation of the mechanical properties of UHPFRC
28 using Non-Destructive Testing (NDT) [12-13] and there are not any published studies to date on
29 combined NDT methods for the estimation of the mechanical characteristics of UHPFRC. Washer *et*
30 *al.* [12] investigated the applicability of Ultrasonic Pulse Velocity (UPV) on UHPFRC, and the effect
31 of steel fibres content on the wave velocity. The effectiveness of UPV was also examined by Hassan
32 and Jones [13] and the need for further investigation was highlighted.

33 NDT methods are useful for the evaluation of the condition of structures, by performing indirect
34 assessment of concrete properties. NDT has many advantages as structural damage during testing is
35 reduced, is relatively simple and less time consuming, and there is possibility of taking measurements
36 even from structures where cores cannot be drilled [14-15]. NDT methods have also been proposed for
37 the assessment of the damage and for the survey of detailed condition of concrete structures and road
38 pavements [16]. There are several NDT methods and two of the most commonly used for in-situ
39 applications are the Rebound Hammer (RH) and the UPV techniques. RH test is a quick method for
40 determining the quality of concrete based on its surface hardness [17]. Schmidt rebound hammer is
41 used to measure the hardness of the surface. Schmidt hammer consists of a mass and a spring which is
42 sliding along a bar which impacts on the end of a steel plunger. After the impact on the concrete
43 surface, the mass rebounds from the steel plunger and moves an index rider. Schmidt hammers
44 normally measure either R-value or Q-value. R-value is the rebound index which is being calculated
45 by the ratio of paths of the mass before and after impact. Q-value or coefficient of restitution is the
46 ratio of kinetic energies of the mass before and after the impact. The energy absorbed by the concrete
47 depends on the stress-strain characteristics of concrete and hence on the modulus of Elasticity and the
48 maximum compressive strength. UPV method [18-19] is based on measurements of the velocity of an
49 ultrasonic pulse which is generated by an electro-acoustical transducer through concrete. Using UPV
50 results, the structure of concrete alongside with its density and any cracks or defects can be evaluated.
51 In the literature, there are various proposed models for conventional concrete for the correlation of RH
52 index values and UPV with concrete compressive strength and modulus of Elasticity [26, 38-39]. In
53 the last few years, combination of more than one method is becoming more popular since they can
54 offer improved reliability and limited errors compared to respective results of individual methods [21,
55 40-44]. SonReb method is one of them. The term SonReb is created by combing the terms ‘Sonic’ and
56 ‘Rebound’ and is a method which is based on the combination of UPV and RH tests results; and until
57 now has only been used for the development of models appropriate for the prediction of conventional
58 concrete compressive strength. This combined method is more accurate than the single NDT methods
59 as takes into consideration two parameters (UPV and RH) which are influenced in different ways by
60 similar factors related to concrete density and hardness. The SonReb method is an empirical method to
61 determine appropriate models for the correlation of the mechanical characteristics (normally
62 compressive strength) with the UPV and RH index values. By using multiple-regression analysis, the
63 mechanical characteristics of the examined material is expressed as a function of the average RH and
64 UPV values and there are published models in the literature for the estimation of the compressive
65 strength of conventional concrete [45-48].

66 To date there are very limited studies on the use of NDT techniques for the evaluation of the
67 mechanical performance of UHPFRC [12-13] and there are not any published studies on combined
68 NDT methods (i.e. SonReb). The main aim of this study is to evaluate the reliability of NDT methods
69 for the assessment of the mechanical characteristics (compressive strength and modulus of Elasticity)
70 of UHPC and UHPFRC. Various mixes have been examined, with and without steel fibres (UHPFRC

71 and UHPC), and compressive and tensile tests have been conducted alongside with RH and UPV tests
72 at different ages. The application of established relationships for the correlation of the dynamic
73 modulus of Elasticity with the UPV for homogeneous isotropic elastic medium have been examined
74 [12, 13] and the results have been compared to the experimental values. The experimental results have
75 been used for the development of NDT models using UPV, RH and combination of UPV and RH
76 (SonReb) values.

77 2. Experimental procedure

78 2.1 Preparation of UHPFRC

79 In the current study, three different mixes have been examined; one using 1% steel fibres (UHPFRC-
80 1), one using 3% steel fibres (UHPFRC-3) and another one without steel fibres (UHPC). UHPFRC
81 mix design is based on previous studies [5, 7] where 2% and 3% (by volume of the mix) steel fibres
82 have been used. In the current study the selection of the three mix designs of Table 1 (0%, 1% and 3%
83 steel fibres) has been made in order to evaluate the effect of the steel fibres quantity by comparing the
84 results of mixes without steel fibres (UHPC), with low (UHPFRC-1) and with relatively high
85 percentage of steel fibres (UHPFRC-3). All three concrete mix designs are presented in Table 1.

86 Silica fume, silica sand, Ground Granulated Blast Furnace Slag (GGBS), and cement class 32.5 R type
87 II have been used together with polycarboxylate superplasticizer. Steel fibres with 13 mm length,
88 diameter 0.16 mm, tensile strength 3000 MPa, and modulus of Elasticity equal to 200 GPa have also
89 been incorporated in the UHPFRC mixes.

90 Regarding the mixing method, high-shear pan mixer (Zyklos ZZ 75 HE) has been used for all the
91 examined mixes. Dry ingredients have been mixed first, and then superplasticizer has been added in
92 the mix followed by the gradual addition of steel fibres through sieving. All specimens have been
93 placed in a water curing tank until the testing day.

94 Cubic specimens with dimension 100 mm have been tested under compression alongside with
95 nondestructive tests (RH and UPV) at 1, 2 (for UHPFRC-1 only), 3, 7 14 (for UHPFRC-1 only), and
96 28 days after casting. For the evaluation of the modulus of Elasticity and the tensile strength, dog-bone
97 specimens have been cast and tested at 1, 2 (for UHPFRC-1 only), 3, 7 and 28 days. These testing ages
98 have been selected in order to obtain a wide range of experimental results which will be able to be
99 used for the regression analyses and for the development of empirical models. Three specimens have
100 been tested for each mix and for all the examined ages. Geometry of dog-bone specimens is illustrated
101 in Fig. 1a and cube and dog-bone samples after casting are presented in Fig. 1b.

102 2.2 Mechanical and Non-Destructive Testing

103 The compressive strength tests were carried out using an Avery Denison compressive testing
104 machine and the tests were conducted in accordance with BS EN 12390-3:2009 [49] with a
105 loading rate of 0.6 MPa/sec (Fig. 2a). For the tensile testing of the dog-bone shaped
106 specimens, tests under displacement rate of 0.007 mm/s were conducted using an Instron

107 universal testing machine. Linear Variable Differential Transformer (LVDT) and a special
108 setup designed in order to measure the average of the extensions of the two sides of the
109 specimens (Fig. 2b) [8]. The accuracy of the strain measurements has been validated using
110 Digital Image Correlation (DIC) system and these values together with the load recordings
111 have been used for the evaluation of the modulus of Elasticity values.

112 For the rebound hammer testing, nine impacts were conducted at each specimen and the median value
113 was calculated as proposed by IS 13311 [18] and BS EN 12504-2 [50]. SilverSchmidt concrete
114 rebound hammer was used in the current study. Tests were conducted on the moulded surfaces and all
115 readings were taken at a distance not nearer on edge than 20 mm and not less than 20 mm from each
116 other [17, 18] and the square of the coefficient of restitution values (Q-values) have been recorded. For
117 the UPV measurements, Pundit Lab was used and the two transducers were placed on opposite sides
118 of the cubes using a thin layer of couplant at the interface between the transducers and the specimens
119 as proposed by BS 1881-203 [19] for the determination of pulse velocity by direct transmission. Three
120 specimens have been examined for each mix for all the examined ages and these results have been
121 used to correlate NDT characteristics to the respective compressive strength values.

122 2.2.1 Mechanical testing results

123 The development of compressive and tensile strength with the age of the specimens for the mixes with
124 and without steel fibres, are presented in Fig. 3 and 4.

125 Results of Fig.3 indicate that, as expected, addition of 3% of steel fibres leads to an increment of
126 compressive strength values which is clear after 7 days of curing and is almost 5%.

127 From the results of Fig.4 it is obvious that modulus of Elasticity and tensile strength are increased with
128 the age of the specimens in all three mixes while the modulus of Elasticity values are not considerably
129 affected by the addition of steel fibres. It is also evident that addition of 3% of steel fibres leads to a
130 significant improvement of the post-cracking performance of the material. The slope of the initial
131 linear part of the stress strain distributions (Fig. 4) have been used for the calculation of the modulus
132 of Elasticity of the various mixes at all the examined ages. From the experimental results for the mix
133 design without steel fibres (UHPC), seven modulus of Elasticity values have been calculated since in
134 some of the examined specimens the failure occurred near the grips of the testing machine and these
135 results have been eliminated from the calculations. For UHPFRC-1, thirteen modulus of Elasticity
136 values have been calculated since two tests has been eliminated for the same reason. In case of
137 UHPFRC-3 where high percentage of fibres has been used, all 12 tests have been successfully tested
138 and all the results have been used for the calculation of modulus of Elasticity values.

139 2.2.2 Application of theoretical model for homogeneous elastic medium

140 The application of elastodynamic theory has been investigated and the reliability of the examined
141 models has been validated using the experimental data. Based on previous studies [12, 13] the

142 application of the established relationships for the correlation of the dynamic modulus of Elasticity
 143 ($E_{d,u}$) and the UPV for homogeneous isotropic elastic medium are appropriate for the estimation of
 144 the elastic properties of UHPFRC since the material exhibits isotropic elastic behaviour [12, 13].
 145 The theory of an ultrasonic pulse travelling in a homogenous isotropic elastic medium has been
 146 adopted in this study in order to correlate compressive wave velocity ($V_{p,s}$) with dynamic modulus of
 147 Elasticity ($E_{d,u}$), density (ρ), and Poisson's ratio (ν_u) (Eq. 1) [51]. The model proposed by BSI CP110:
 148 [52] has been used to calculate the static modulus of Elasticity (E_{cm}) from the dynamic modulus of
 149 Elasticity ($E_{d,u}$) (Eq. 2). The compressive strength (f_c) has also been calculated from the values of the
 150 static modulus of Elasticity (E_{cm}) using the model proposed by Eurocode 2 (Eq. 3) [53].

151

$$V_{p,s} = \sqrt{\frac{E_{d,u} (1-\nu_u)}{\rho (1+\nu_u)(1-2\nu_u)}} \quad (1)$$

$$E_{cm} = 1.25E_{d,u} - 19 \quad (2)$$

$$E_{cm} = 9500*(f_c)^{1/3} \quad (3)$$

152

153 Eq. 1-3 have been used to calculate static modulus of Elasticity (E_{cm}) and compressive strength using
 154 the ultrasonic wave velocity values ($V_{p,s}$). In the current study average Poisson's ratio value of $\nu_u=0.2$
 155 has been used [13] while the density values which are based on experimental measurements have been
 156 taken equal to 2187 kg/m³ for UHPC, 2244 kg/m³ for UHPFRC-1, and 2357 kg/m³ for UHPFRC-3.
 157 Using these parameters, the static modulus of Elasticity has been calculated using Eq. 1-2 and the
 158 results are compared with the respective experimental values (Fig. 5).

159 The results of Fig. 5 have been used for the calculation of the error (%) in the modulus of Elasticity
 160 values (E_{cm}) calculated for UHPC, UHPFRC-1 and UHPFRC-3. The distribution of the error (%) with
 161 the different values of the modulus of Elasticity is presented in Fig. 6.

162 The results of Fig. 6 indicate that overall the error is reduced as the modulus of Elasticity values are
 163 increased. This can be attributed to the fact that Eq. 2 have been derived for conventional concrete and
 164 calibration of this model is required for the calculation of the early-age characteristics.

165 The theoretical results for the modulus of Elasticity and Eq.3 have been used for the calculation of the
 166 compressive strength values and these results are compared with the respective experimental results
 167 (Fig. 7).

168 The results presented in Fig. 7 indicate that application of elastodynamic theory together with Eq. 3
 169 cannot accurately predict the actual compressive strength values of UHPFRC. This is attributed to
 170 limitation of Eq. 2 and Eq. 3 which have been empirically calculated based on data for conventional
 171 concrete. Also based on the results of Fig. 7, it is evident that the theoretical equations lead the
 172 considerably lower values compared to the experimental results. The theoretical values are lower than
 173 half of the respective experimental values and the deviation between the experimental and the

174 theoretical values is not considerably affected by the percentage of the steel fibres since it is almost the
175 same for UHPC, UHPFRC-1 and UHPFRC-3. In the following sections, the development of
176 appropriate empirical relationships for the calculation of the compressive strength and the modulus of
177 Elasticity based on the NDT results will be presented.

178 2.2.3 Non-destructive results versus mechanical testing: Empirical models

179 In this section, empirical relationships between the results of mechanical and non-destructive tests,
180 have been developed. Empirical models for conventional concrete have been proposed in previous
181 studies for the calculation of the compressive strength using RH and UPV measurements where
182 experimental results have been used and best fit lines have been calculated [26, 38]. Also, the strong
183 correlation between the modulus of Elasticity (E_{cm}) and the UPV has been highlighted in a previous
184 study where the use of empirical models for the calculation of E_{cm} of conventional and sub-standard
185 concretes has been proposed as a simplified method [39]. Linear and exponential regression models
186 have been examined in the current study for the evaluation of the compressive strength and modulus of
187 Elasticity.

188 2.2.3.1 RH and UPV versus compressive strength results-Linear and Exponential models

189 The relationship between Q and compressive strength values together with the linear and exponential
190 regression models and the coefficient of determination (R^2) for UHPC (without steel fibres),
191 UHPFRC-1 and UHPFRC-3 are presented in Fig. 8a, Fig. 8b and Fig. 8c respectively.

192 According to the results of Fig. 8, high coefficient of determination values for both linear and
193 exponential regression models have been found for all the examined cases. In both linear and
194 exponential regression models, the coefficient of determination has been found to be in the range 0.94-
195 0.98. In case of the mix without steel fibres (UHPC), similar values of the coefficient of determination
196 for linear and exponential models have been obtained (0.94 and 0.95). For specimens with 1 % steel
197 fibres (UHPFRC-1), higher coefficient of determination have been observed for linear regression
198 model while for specimens with 3% steel fibres (UHPFRC-3), higher value of the coefficient has been
199 observed for exponential regression.

200 The compressive strength results versus UPV are presented in Fig. 9 together with respective linear
201 and exponential regression models for UHPC, UHPFRC-1 and UHPFRC-3. The results indicate that in
202 all the examined cases, exponential regression models have been found to have very high values
203 almost equal to unity (0.99-1.00). In case of linear regression models, the coefficients of determination
204 were found to be in the range 0.90-0.97 (Fig. 9).

205 In the following section, NDT results are compared to the modulus of Elasticity values and respective
206 empirical linear and exponential models have been calculated.

207

208 2.2.3.2 RH and UPV versus modulus of Elasticity results-Linear and Exponential models

209 Similar investigation to the one presented in section 2.2.3.2 has been conducted for the modulus of
210 Elasticity with the UPV and RH results. Linear and exponential regression models have been
211 calculated for Q and UPV values for UHPC, UHPFRC-1 and UHPFRC-3 and the results are presented
212 in Fig. 10.

213 The results of the modulus of Elasticity with the respective Q-values indicate that the coefficient of
214 determination (R^2) values are lower compared to the values calculated for compressive strength and in
215 the range of 0.78-0.94. Higher R^2 values have been observed for exponential regression models for
216 UHPC and UHPFRC-3, while for UHPFRC-2 R^2 value is higher for the linear model. The highest R^2
217 value (0.94) has been obtained for the mix without steel fibres (UHPC) and for exponential model.

218 Modulus of Elasticity versus UPV results and linear and exponential regression lines for all the three
219 mixes are presented in Fig. 11. The results indicate that the exponential regression models have been
220 found to lead to higher coefficient of determination values for all the examined specimens apart from
221 UHPFRC-1 where R^2 value for linear model (0.97) is slightly higher compared to the respective value
222 for the exponential model (0.95). It is also worth mentioning that in this case (Fig. 11) very high R^2
223 values (0.82-0.95) have been observed for all the examined specimens for exponential models.

224 2.2.4 Combined SonReb method

225 All the experimental results presented in section 2.2.1 (Q-values, UPV values, compressive strength
226 and Modulus of Elasticity test results) have been used to determine SonReb curve coefficients for both
227 mixes with and without steel fibres (UHPFRC and UHPC). Eq. 4 is the general equation which has
228 been used to correlate compressive strength and modulus of Elasticity with UPV and Q-values.

$$F = a V^b S^c \quad (4)$$

229 where:

F is the mechanical characteristic (compressive strength or Modulus of Elasticity,

V is the ultra-sonic pulse velocity,

S is the Q-value from the rebound hammer tests, and

a, b, c are constants depended on the material.

230

231 The natural logarithms of the data of Fig. 8 and Fig. 9 have been initially calculated, and then
232 'LINEST' function in Microsoft Excel has been used to calculate straight lines to best fit the data
233 using the 'least squares' following the procedure proposed by Proceq [54]. Based on these analyses,
234 appropriate values for coefficients a, b, c for the compressive strength of UHPC and UHPFRC 1 and
235 UHPFRC 3 have been determined (Table 2). Also, the respective values proposed by RILEM 43-CND
236 [45] for standard concretes are presented in the same table.

237 The same analyses have been conducted for the modulus of Elasticity using the results presented in
238 Fig. 9 and Fig. 10 and SonReb coefficients for the modulus of Elasticity are presented in Table 3.

239 The SonReb models with the coefficients calculated in this study (Tables 2 and 3) have been applied
240 for various UPV and Q values and the results of the compressive strength and modulus of Elasticity
241 are presented in Fig. 12a and Fig. 12b respectively.

242 From the results of Fig. 12 it is obvious that as expected, compressive strength and modulus of
243 Elasticity are both increased as UPV and Q values are increased. The results show that the trend of the
244 models is almost the same for all the examined mixes but the exact values are highly affected by the
245 various mix designs that have been examined (UHPC, UHPFRC-1, and UHPFRC-2), so appropriate
246 calibration is required for different mixes. Only in case of compressive strength values (Fig. 12a) the
247 results have been found to be quite similar for UHPFRC-1 and UHPFRC-3 mixes.

248 In order to evaluate the empirical models of Table 2, isoresistance curves for all the examined mixes
249 (UHPC, UHPFRC-1 and UHPFRC-3) have been generated and these results have been compared with
250 the respective curves for conventional concrete using the model proposed by RILEM 43-CND [45]
251 (table 2). The isoresistance curves for all the examined models are presented in Fig. 13.

252 From the results of Fig. 13 it is evident that the mix design is considerably affecting the shape of the
253 isothermal curves. For high performance mix design without steel fibres (UHPC) an abrupt drop of the
254 Q-Value is observed as UPV is increased, while as the fibre percentage is increased (UHPFRC-1 and
255 UHPFRC-3), this drop becomes more gradual. The shapes of the models for UHPFRC-1 and
256 UHPFRC-3 are similar to the shape of RILEM 43-CND [45] model for the examined range of values
257 (Fig. 13). However it is clear that RILEM 43-CND [45] model for conventional concrete leads to
258 considerably lower compressive strength values. This is attributed to the special mixture composition
259 in case of UHPC and UHPFRC and mainly in the high cement content, in the aggregates type (silica
260 sand) and in the addition of admixtures (slag and silica fume used in UHPFRC). These factors are
261 crucial for the parameters of the empirical SonReb models [45]. According to RILEM 43-CND [45]
262 correction factors (coefficients of influence) should be applied in order to calibrate the model for
263 different mix designs. In the examined mixes with UHPFRC-1 and UHPFRC-3 coefficients of
264 influence in the range of 1.5-2 should be used in order to take into account the effect of the special
265 composition of the examined mixes.

266 In the following section (Section 2.3), the accuracy of the calculated SonReb empirical models is
267 compared with the accuracy of the linear and exponential models presented in 2.2.3.1 and 2.2.3.2.

268 **2.3 Evaluation of the accuracy of linear, exponential and combined SonReb models for the** 269 **calculation of compressive strength and modulus of Elasticity values**

270 In order to evaluate the accuracy of all the examined models, the results of the linear, the exponential
271 and the combined SonReb empirical models have been compared with the actual mechanical tests
272 results. The mean values of the calculated results for the various mixes (UHPC, UHPFRC 1, UHPFRC
273 3) at all the examined ages are compared with the respective compressive strength and modulus of

274 Elasticity results obtained from the mechanical testing, and the comparisons are presented in Fig. 14
275 and Fig. 15 together with the diagonal line (line of equality) which represents absolute equality.

276 The results of Fig. 14 and Fig. 15 indicate that in all the examined cases the values calculated with the
277 combined SonReb method are very close to the line of equality for the whole range of the examined
278 values and for both compressive strength and modulus of Elasticity values. In order to quantify the
279 level of accuracy of each method, the % difference (error) between the predicted value using each of
280 the methods and the respective actual value obtained from mechanical tests, has been calculated. In
281 Fig. 16 and Fig. 17, errors (%) versus actual mechanical characteristics obtained from the mechanical
282 tests are presented for each mix design.

283 From the compressive strength results presented in Fig. 16, it is obvious that the lowest error values
284 for UHPC and UHPFRC-1 have been achieved for the combined SonReb. For UHPFRC-3 the lowest
285 error values for compressive strength values up to 75 MPa have been calculated using Exponential-Q
286 while for higher strength values SonReb and Exponential-V models have been found to be the most
287 accurate ones. For all the examined cases the error (%) values of SonReb method have been found to
288 be below 10%. Overall the highest error values have been observed for the Exponential-Q and Linear-
289 V models for UHPC and UHPFRC-1, while for UHPFRC-3, Linear-V and Linear-Q have been found
290 to give the highest error values. Exponential-V model has been found to give very low error values
291 and below 10% in case of UHPFRC-1 and UHPFRC-3. However, the error value was quite high and
292 exceeded 10% in case of mix design without steel fibres (UHPC).

293 Regarding the modulus of Elasticity results (Fig. 17), overall the most accurate values have been
294 calculated with the combined SonReb method. All the error values of SonReb method have been
295 found to be below 1.2% for UHPC, below 5.7% for UHPFRC-1, and below 8.6% for UHPFRC-3 for
296 modulus of Elasticity values lower than 30 MPa while for higher values the error has not exceeded
297 1%. Exponential-Q models have been found to lead to very low error values and below 5.7% for
298 UHPC and UHPFRC-3 mixes, but high error values in the range of 5.9-19.0% have been observed for
299 UHPFRC-1. The highest error values overall have been observed for Linear-Q models.

300 From the observations described above it is evident that the only model which provides accurate
301 results with low error values (below 10%) in all the examined cases is SonReb. For all the other
302 models, there are variations in the degree of accuracy depending on the mix design and the special
303 characteristics of each specimen. This is attributed to the random distribution of the various
304 components of the mix and especially to the dispersion of the steel fibres which leads to a variation in
305 the properties of the materials and especially at the surface of the material. Parameters such as the
306 mixing procedure and the vibration of the material can considerably affect the characteristics of the
307 outer surface and subsequently its hardness. In this case, Rebound Hammer (RH) measurements which
308 are mainly affected by the hardness of the surface are not sufficient for the accurate evaluation of the
309 mechanical characteristics of the material, and combination with UPV measurements (i.e. SonReb) is

310 essential in order to obtain accurate models for both compressive strength and the modulus of
311 Elasticity of UHPFRC mixes. This is evidenced by all the results presented in the current study.

312 3 Conclusions

313 In the current study, the reliability of NDT methods for the evaluation of the compressive strength and
314 the modulus of Elasticity of UHPC and UHPFRC has been investigated. Ultrasonic Pulse Velocity
315 (UPV), Rebound Hammer (RH) and combined SonReb techniques have been examined and various
316 models have been developed and evaluated using actual mechanical characteristics obtained from the
317 mechanical tests. Also, the reliability of theoretical models for homogenous elastic medium for the
318 calculation of the modulus of Elasticity of UHPC and UHPFRC using UPV measurements has been
319 evaluated.

320 Based on the findings of this investigation, the following conclusions have been drawn.

321 Effect of steel fibres on mechanical characteristics of UHPFRC:

- 322 • Based on the mechanical testing, the compressive strength of UHPFRC with 3% steel fibres is
323 slightly higher (almost 5%) compared to the respective values obtained for UHPC (without
324 steel fibres).
- 325 • Modulus of Elasticity is not considerably affected by the addition of steel fibres, while the
326 post-cracking response of the material is significantly enhanced as the steel fibres percentage
327 is increased.

328 Evaluation of the examined NDT techniques:

- 329 • From the application of the theoretical models for homogenous elastic medium it has been
330 observed that the static modulus of Elasticity cannot be accurately predicted especially for
331 relatively low values, due to the fact that Eq. 2 has been empirically calculated based on data
332 for conventional concrete. Also, the application of the theoretical model (Eq. 1) together with
333 the empirical relationships (Eq. 2 and Eq. 3) lead to considerably lower compressive strength
334 values compared to the respective experimental results.
- 335 • From the correlation of compressive strength with NDT values, high coefficient of
336 determination values (0.94-0.98) for both linear and exponential regression models have been
337 found for Q-values versus compressive strength. From the distribution of UPV with
338 compressive strength results, coefficient of determination values in the range of 0.90-0.94
339 have been found for linear regression models, while significantly higher are the respective
340 values (0.98-0.99) for exponential regression models.
- 341 • Regarding the Q versus modulus of Elasticity values, lower regression values compared to the
342 respective results for the compressive strength have been calculated for both linear and
343 exponential models (0.81-0.88 for linear regression models and 0.78-0.94 for exponential
344 models). From the correlation of UPV with the modulus of Elasticity, coefficients of

345 determination in the range of 0.71-0.97 have been calculated for linear regression values,
346 while overall higher values (0.82-0.95) have been achieved for exponential models.

- 347 • Isoresistance curves for the proposed models for UHPC, UHPFRC-1, UHPFRC-3 have been
348 compared with the proposed model by RILEM 43-CND [45] for conventional concrete. From
349 these results it has been found that the shape of the isothermal curves is considerably affected
350 by the mixes. The trend of the results of the models for UHPFRC-1 and UHPFRC-3 is similar
351 to the trend of RILEM 43-CND [45] model but it is evident that the RILEM 43-CND [45]
352 model leads to considerably lower compressive strength values. Correction factors
353 (coefficients of influence) should be applied in order to take into account the differences in the
354 mixtures' composition. In case of UHPFRC-1 and UHPFRC-3 appropriate values for the
355 coefficients of influence have been found to be in the range of 1.5-2.
- 356 • From the evaluation of all the models presented for the compressive strength, it has been
357 found that overall the lowest error values have been achieved for the combined SonReb and in
358 all the examined cases error below 10% has been achieved.
- 359 • Regarding the modulus of Elasticity, overall SonReb method has been found to be the most
360 accurate method. In case of UHPC, error values below 1.2% have been obtained. Based on the
361 results of UHPFRC-1, the error has not exceeded 5.7%. The respective maximum error value
362 for UHPFRC-3 has been found to be equal to 8.6% for modulus of Elasticity values lower
363 than 30MPa, while for higher values the error has not exceeded 1%.

364 The main conclusion of this study is that the combined SonReb method can offer high level of
365 accuracy since in all the examined cases error below 10% has been achieved. Hence, SonReb method
366 is highly recommended for the reliable prediction of the compressive strength and modulus of
367 Elasticity of UHPC and UHPFRC. The models that have been proposed in the current study have been
368 calculated for plain (without steel fibres) UHPC and for UHPFRC with 1% and 3% steel fibres.
369 Similar procedure is proposed for the development of appropriate models for UHPFRC with different
370 mix design and other steel fibres content.

371

372 **Acknowledgments**

373 The authors would like to greatly acknowledge Sika Limited and Hanson Heidelberg Cement Group
374 for providing raw materials for the experimental part of this study. Also, the authors would like to
375 express their gratitude to the anonymous reviewers for their comments who have led to significant
376 improvement of the quality of the paper.

377

378 **References**

- 379 [1] B.A. Graybeal, Material property characterization of ultra-high performance concrete,
380 Federal Highway Administration (2006).
- 381 [2] S.T. Kang, Y. Lee, Y.D. Park, J.K. Kim, Tensile fracture properties of an Ultra High Performance
382 Fiber Reinforced Concrete (UHPFRC) with steel fiber, *Composite Structures*, 92(1) (2010) 61–
383 71.
- 384 [3] Y. Yoo, H.O. Shin, J.M. Yang, Y.S. Yoon, Material and bond properties of ultra high performance
385 fiber reinforced concrete with micro steel fibers, *Composites Part B: Engineering*, 58 (2013)
386 22–133.
- 387 [4] S.T. Kang, J.K. Kim, The relation between fiber orientation and tensile behavior in an Ultra High
388 Performance Fiber Reinforced Cementitious Composites (UHPFRCC), *Cement and Concrete
389 Research*, 41(10) (2011) 1001–1014.
- 390 [5] A. Hassan, S. Jones, G. Mahmud, Experimental test methods to determine the uniaxial tensile and
391 compressive behaviour of ultra-high performance fibre reinforced concrete (UHPFRC),
392 *Construction and Building Materials*, 37 (2012) 874–882.
- 393 [6] R. Toledo Filho, E. Koenders, S. Formagini, E. Fairbairn, Performance assessment of ultra-high
394 performance fibre reinforced cementitious composites in view of sustainability, *Materials &
395 Design*, 36 (2012) 880–888.
- 396 [7] A.P. Lampropoulos, S.A. Paschalis, O.T. Tsioulou, S.E. Dritsos, Strengthening of reinforced
397 concrete beams using ultra high performance fibre reinforced concrete (UHPFRC), *Engineering
398 Structures*, 106 (2016) 370-384.
- 399 [8] A.P. Lampropoulos, S.A. Paschalis, Ultra High Performance Fiber Reinforced Concrete Under
400 Cyclic Loading, *ACI Material Journal*, 113 (2016) 419-427.
- 401 [9] D. Nicolaides, A. Kanellopoulos, P. Savva, and M. Petrou, Experimental field investigation of
402 impact and blast load resistance of Ultra High Performance Fibre Reinforced Cementitious
403 Composites (UHPFRCCs), *Construction and Building Materials*, 95 (2015) 566-574.
- 404 [10] BFUP AFGC, Ultra high performance fibre-reinforced concretes, Interim
405 recommendations, AFGC/SETRA Working Group, France (2002).
- 406 [11] A.A. Shah, Y. Ribakov, Recent trends in steel fibered high-strength concrete, *Materials
407 & Design*, 32(8–9) (2011) 4122–4151.
- 408 [12] G. Washer, P. Fuchs, B.A. Graybeal, J.L. Hartmann, Ultrasonic testing of reactive powder
409 concrete, *IEEE Trans Ultrason Ferroelectr Frequency Control*, 51(2) (2004) 193–201.

- 410 [13] A. Hassan, S. Jones, Non-destructive testing of ultra high performance fibre reinforced concrete
411 (UHPRFC): A feasibility study for using ultrasonic and resonant frequency testing techniques,
412 Construction and Building Materials, 35 (2012) 361-367.
- 413 [14] V. M. Malhotra, Testing Hardened Concrete: Non-destructive Methods, ACI, monograph No. 9,
414 Detroit (1976).
- 415 [15] A. Leshchinsky, Non-destructive methods instead of specimens and cores, quality control of
416 concrete structures, International Symposium Held by RILEM. Belgium (1991).
- 417 [16] K. Themistocleous, K. Neocleous, K. Pilakoutas, D. G. Hadjimitsis, Damage assessment using
418 advanced non-intrusive inspection methods: integration of space, UAV, GPR, and field
419 spectroscopy, in: Second International Conference on Remote Sensing and Geoinformation of the
420 Environment, Pafos, 2014, 7-10 April, 2014.
- 421 [17] BS1881-202, Recommendations for surface hardness testing by rebound hammer, BSI, UK
422 (1986).
- 423 [18] IS 13311 (Part I): 1992 Non-Destructive Testing of Concrete Methods of test(Ultrasonic Pulse
424 Velocity), BIS, New Delhi (1992).
- 425 [19] BS 1881-203, Recommendations for measurement of velocity of ultrasonic pulses in concrete,
426 BSI, UK (1986).
- 427 [20] I.N. Prassianakis, P. Giokas, Mechanical properties of old concrete using destructive and
428 ultrasonic non-destructive testing methods, Magazine of Concrete Research, 55 (2003) 171-176.
- 429 [21] J.H. Bungey, The validity of ultrasonic pulse velocity testing of in-place concrete for strength,
430 N.D.T. International 13(6) (1980) 296-300.
- 431 [22] I. Facaoaru, Contribution à l'étude de la relation entre la résistance du béton à la compression et
432 de la vitesse de propagation longitudinale des ultrasons, RILEM 22 (1961) 125-154. (in French)
- 433 [23] K.G. Trezos, K. Georgiou, C. Marebelias, Determination of the in situ strength of concrete using
434 the indirect methods of impact and the ultrasounds, Technika Chronika-Scientific Edition TCG
435 13 (1993) 27-41.
- 436 [24] D. Mikulic, Z. Pause, V. Ukrainc, Determination of concrete quality in a structure by combination
437 of destructive and non-destructive methods, Materials and Structures 25 (1992) 65-69.
- 438 [25] L. Logothetis, Combination of three non-destructive methods for the determination of the strength
439 of concrete, PhD Thesis, National Technical University of Athens (1979).
- 440 [26] H.Y. Qasrawi, Concrete strength by combined non-destructive methods simply and reliably
441 predicted, Cement and Concrete Research, 30 (2000) 739-746.

- 442 [27] R.S. Ravindrarajah, Y.H. Loo and C.T. Tam, Recycled concrete as fine and coarse aggregates in
443 concrete, Magazine of Concrete Research, 39 (1987) 214-220.
- 444 [28] A. Goncalves, In situ concrete strength estimation. Simultaneous use of cores, rebound hammer
445 and pulse velocity, International Symposium NDT in Civil Engineering, Germany (1995) 977-
446 984.
- 447 [29] T. Soshiroda, K. Voraputhaporn, Recommended method for earlier inspection of concrete quality
448 by non-destructive testing, Concrete Durability and Repair Technology (1999) 27-36.
- 449 [30] K.K. Phoon, T.H. Wee, C.S. Loi, Development of statistical quality assurance criterion for
450 concrete using ultrasonic pulse velocity method, ACI Material Journal, 96 (5) (1999) 568-573.
- 451 [31] R.H. Elvery, LAM. Ibrahim, Ultrasonic assessment of concrete strength at early ages, Magazine
452 of Concrete Research, (1976) 181-190.
- 453 [32] G.V. Teodoru, The use of simultaneous nondestructive tests to predict the compressive strength of
454 concrete, ACI SP-112, (1998) 137-152.
- 455 [33] Y. Tanigawa, K. Baba, H. Mori, Estimation of concrete strength by combined nondestructive
456 testing method, ACI SP 82, (1984) 57-76.
- 457 [34] W.E. Parker, Pulse velocity testing of concrete, Proceedings - American Society for Testing
458 Materials, 53 (1953) 1033-1042.
- 459 [35] C.H. Yun, K.R. Choi, S.Y. Kim, Y.C. Song, Comparative evaluation of nondestructive test
460 Methods for in-place strength determination, ACI SP 112 (1988) 111-136.
- 461 [36] L.M. Rio, A. Jimenez, F. Lopez, F.J. Rosa, M.M. Rufo, J.M. Paniagua, Characterization and
462 hardening of concrete with ultrasonic testing, Ultrasonics, 42 (2004) 527-530.
- 463 [37] E. Arioglu, N. Arioglu, Testing of concrete core samples and evaluations, Evrim Publisher,
464 Istanbul (1998).
- 465 [38] G.F. Kheder, A two stage procedure for assessment of in-situ concrete strength using combined
466 non-destructive testing. Materials and Structures, 32 (1998) 410-417.
- 467 [39] H. Yildirim, O. Sengul, Modulus of elasticity of substandard and normal concretes. Construction
468 and Building Materials, 25 (2011) 1645-1652.
- 469 [40] M. K. Lim, H. Cao, Combining multiple NDT methods to improve testing effectiveness,
470 Construction and Building Materials, 38 (2013) 1310-1315.
- 471 [41] G. Concu, B. De Nicolo, L. Pani, Non-Destructive Testing as a tool in reinforced concrete
472 buildings refurbishments, Structural Survey, 29 (2) (2011) 147-161.

- 473 [42] D. Breyse, Nondestructive evaluation of concrete strength: an historical review and a new
474 perspective by combining NDT methods, *Construction and Building Materials*, 33 (2012) 139–
475 163.
- 476 [43] I.R. De Almeida, Non-destructive Testing of High Strength Concretes: Rebound (Schmidt
477 Hammer and Ultrasonic Pulse Velocity), *International Symposium held by RILEM, Belgium*
478 (1991) 387- 397.
- 479 [44] G. Kheder, Assessment of in Situ Concrete Strength Using Combined Non-destructive Testing,
480 *First International Arab Conference on Maintenance and Rehabilitation of Concrete Structures*,
481 *Cairo (1998) 59-75*.
- 482 [45] RILEM 43-CND, Combined non-destructive testing of concrete. Draft
483 recommendation for in situ concrete strength determination by combined non-destructive
484 methods, *Materials and Structures*, 26 (1993) 43-49.
- 485 [46] R. Giochetti, L. Lacquaniti, Controlli non distruttivi su impalcati da ponte in calcestruzzo armato,
486 *Nota Tecnica 04, Università degli Studi di Ancona, Facoltà di Ingegneria, Istituto di Scienza e*
487 *Tecnica delle Costruzioni (1980). (in Italian)*
- 488 [47] J. Gasparik, Prove non distruttive in edilizia, *Quaderno didattico A.I.P.n.D., Brescia (1992). (in*
489 *Italian)*
- 490 [48] A. Di Leo, G. Pascale, Prove non distruttive sulle costruzioni in cemento armato, *Convegno*
491 *Sistema Qualità e Prove non Distruttive per l'affidabilità e la sicurezza delle strutture civili,*
492 *Bologna, SAIE'94 (1994). (in Italian)*
- 493 [49] BS EN 12390-3, Compressive Strength of Test Specimens, *Testing Hardened Concrete*, 1-22,
494 *BSI, UK (2009)*.
- 495 [50] BS EN 12504-2, Non-destructive Test. Determination of Rebound Number, *BSI, UK (2001)*.
- 496 [51] R. Jones, *Non-destructive testing of concrete*, London: Cambridge University Press (1962).
- 497 [52] BSI CP110: Part 1, *Code of Practice for the Structural Use of Concrete*, BSI, UK (1972).
- 498 [53] European pre-standard: ENV 1992-1-1: Eurocode 2: Design of concrete structures – Part 1:
499 *General rules and rules for buildings*.
- 500 [54] Proceq, *Using EXCEL to determine SONREB curve coefficients*, Switzerland.

List of tables

Table 1. Mix design of UHPFRC.

Material	Mix proportions (kg/m ³)		
	UHPC	UHPFRC-1	UHPFRC-3
Cement	657	657	657
GGBS	418	418	418
Silica fume	119	119	119
Silica Sand	1051	1051	1051
Superplasticizers	59	59	59
Water	185	185	185
Steel fibres	0	75.2	235.5

Table 2. SonReb coefficients for compressive strength models.

Coefficient	Values calculated for UHPC	Values calculated for UHPFRC-1	Values calculated for UHPFRC-3	Values proposed by RILEM 43-CND [45]
a	2.36E-20	2.78E-11	1.61E-08	2.756E-10
b	5.80	3.00	2.28	2.487
c	0.23	0.92	0.87	1.311

Table 3. SonReb coefficients for modulus of Elasticity models.

Coefficient	Values calculated for UHPC	Values calculated for UHPFRC 1	Values calculated for UHPFRC 3
a	1.12E32	4.05E-11	1.11E16
b	-11.00	3.43	-5.73
c	5.72	-0.37	3.84

List of figures' captions

Fig. 1. a) Geometry of dog-bone specimens and b) dog-bone and cube samples.

Fig. 2. Experimental setup for a) compressive and b) tensile testing of the examined specimens.

Fig. 3. Compressive strength for specimens with and without steel fibres at various ages.

Fig. 4. Tensile strength vs strain at different ages for a) UHPC, b) UHPFRC-1 and c) UHPFRC-3.

Fig. 5. Comparisons between experimental and theoretical values of E_{cm}

Fig. 6. Distribution of error values (%) with the modulus of Elasticity values for UHPC, UHPFRC-1 and UHPFRC-3.

Fig. 7. Comparisons between the theoretical and the experimental results of the compressive strength.

Fig. 8. Correlation of compressive strength with Q-values and respective linear and exponential regression models for a) UHPC, b) UHPFRC-1 and c) UHPFRC-3.

Fig. 9. Correlation of compressive strength with UPV results and respective linear and exponential regression lines for a) UHPC, b) UHPFRC-1 and c) UHPFRC-3.

Fig. 10. Correlation of modulus of Elasticity with Q-values and respective linear and exponential regression lines for a) UHPC, b) UHPFRC-1 and c) UHPFRC-3.

Fig. 11. Correlation of modulus of Elasticity with UPV results and respective linear and exponential regression lines for a) UHPC, b) UHPFRC-1 and c) UHPFRC-3.

Fig. 12. SonReb models a) for compressive strength and b) for modulus of Elasticity for all the examined mixes.

Fig. 13. Isoresistance curves for the proposed models for UHPC, UHPFRC-1, UHPFRC-3 and comparison with RILEM 43-CND [45] model for conventional concrete.

Fig. 14. Correlation between compressive strength values calculated using different models and actual compressive strength values for a) UHPC (without steel fibres), b) UHPFRC-1 and c) UHPFRC-3.

Fig. 15. Correlation between modulus of Elasticity values calculated using different models and actual compressive strength values for a) UHPC (without steel fibres), b) UHPFRC-1 and c) UHPFRC-3.

Fig. 16. Error (%) for all the examined compressive strength models for a) UHPC, b) UHPFRC-1 and c) UHPFRC-3.

Fig. 17. Error (%) for all the examined modulus of Elasticity models for a) UHPC, b) UHPFRC-1 and c) UHPFRC-3.

Fig. 1a

[Click here to download high resolution image](#)

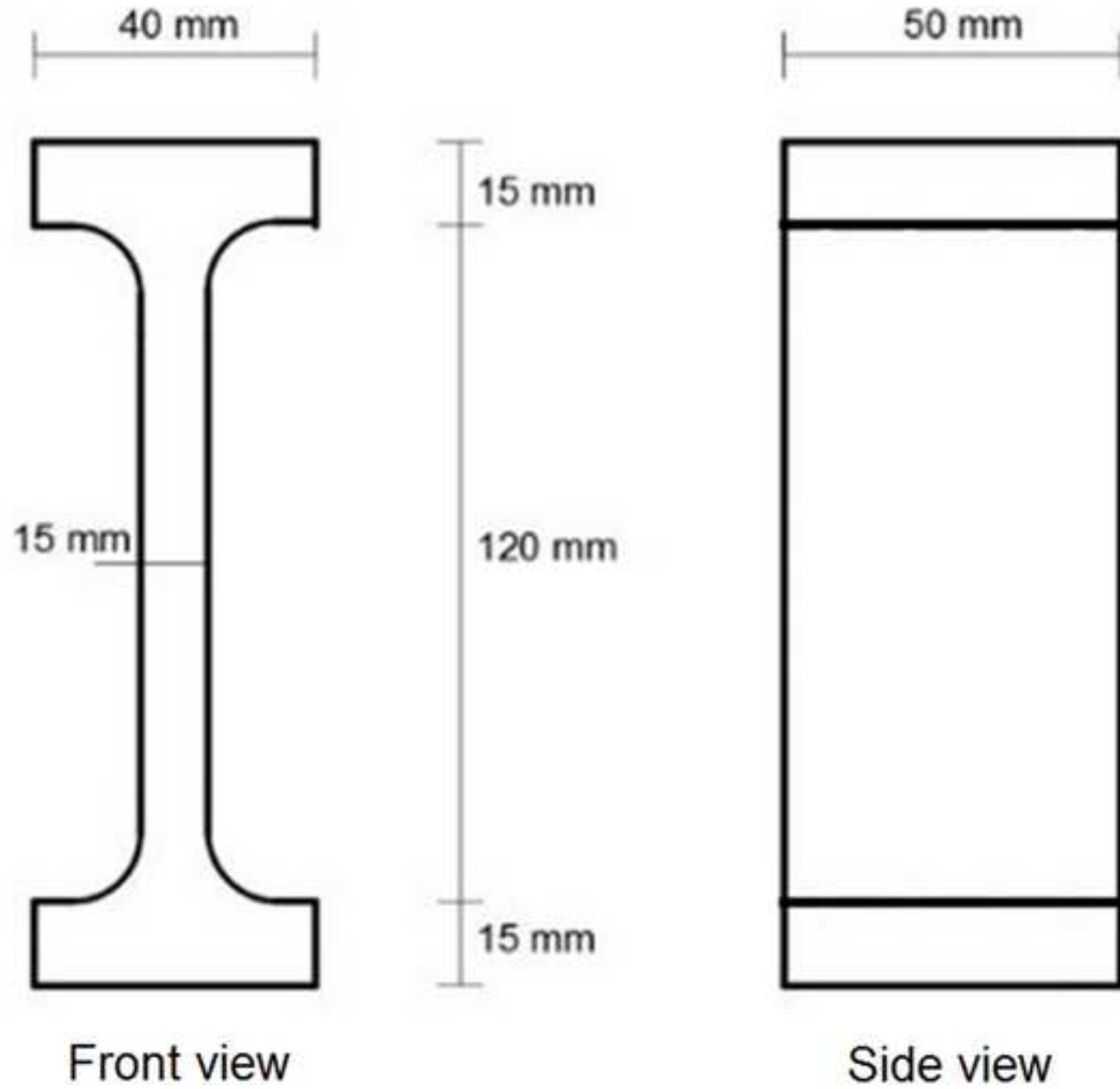


Fig. 1b
[Click here to download high resolution image](#)



Fig. 2a
[Click here to download high resolution image](#)



Fig. 2b

[Click here to download high resolution image](#)



Fig. 3

[Click here to download high resolution image](#)

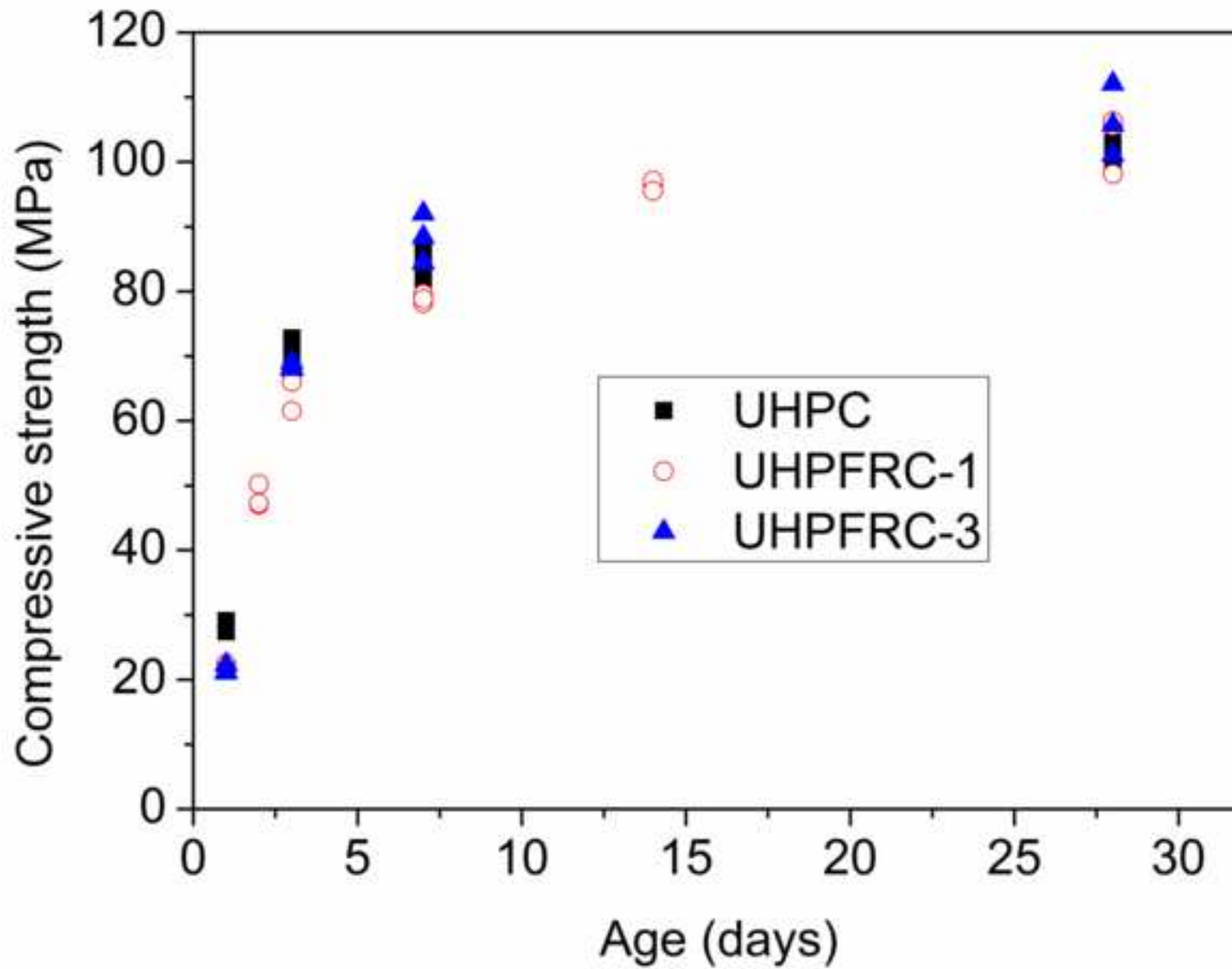


Fig. 4a

[Click here to download high resolution image](#)

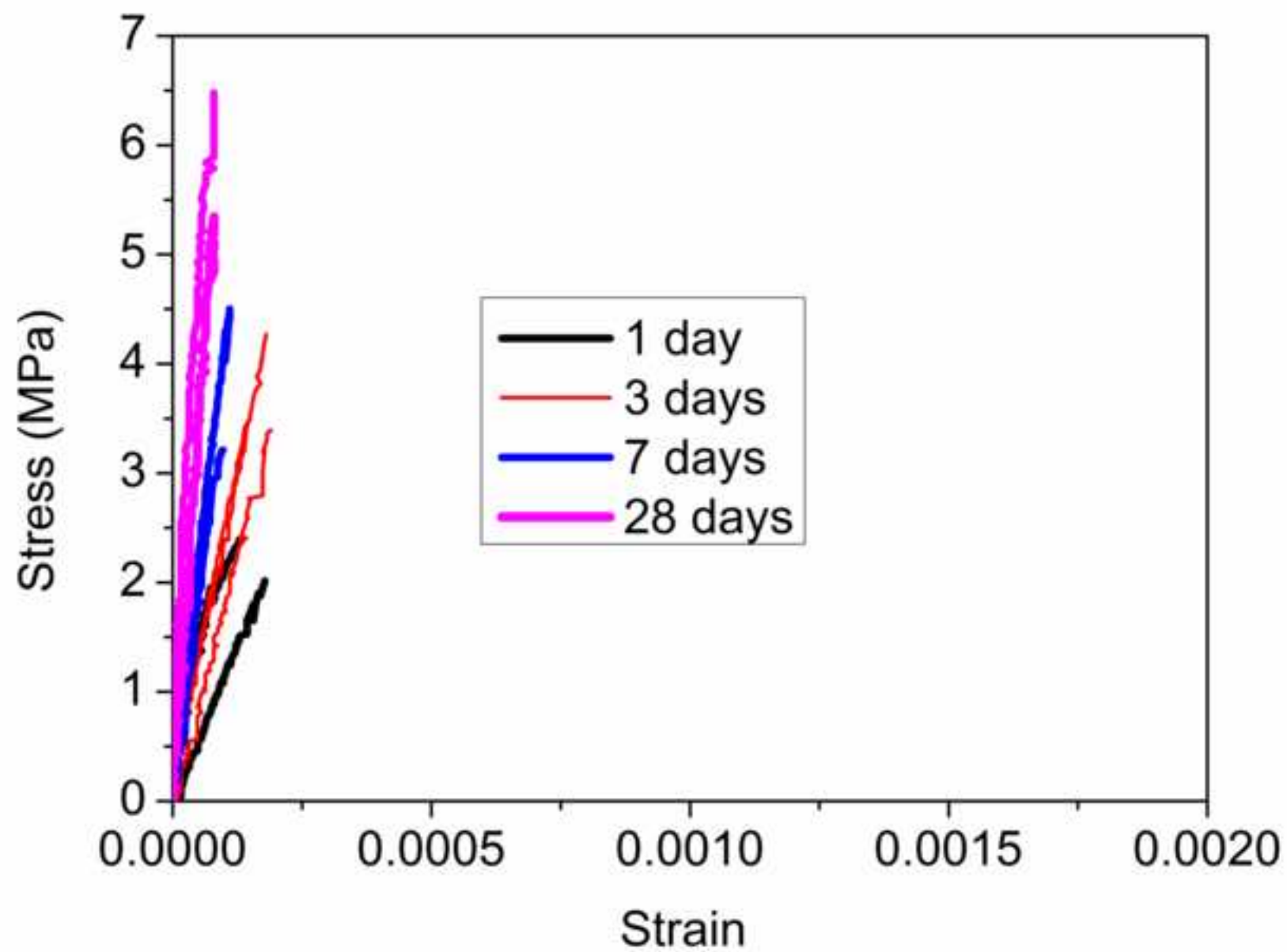


Fig. 4b

[Click here to download high resolution image](#)

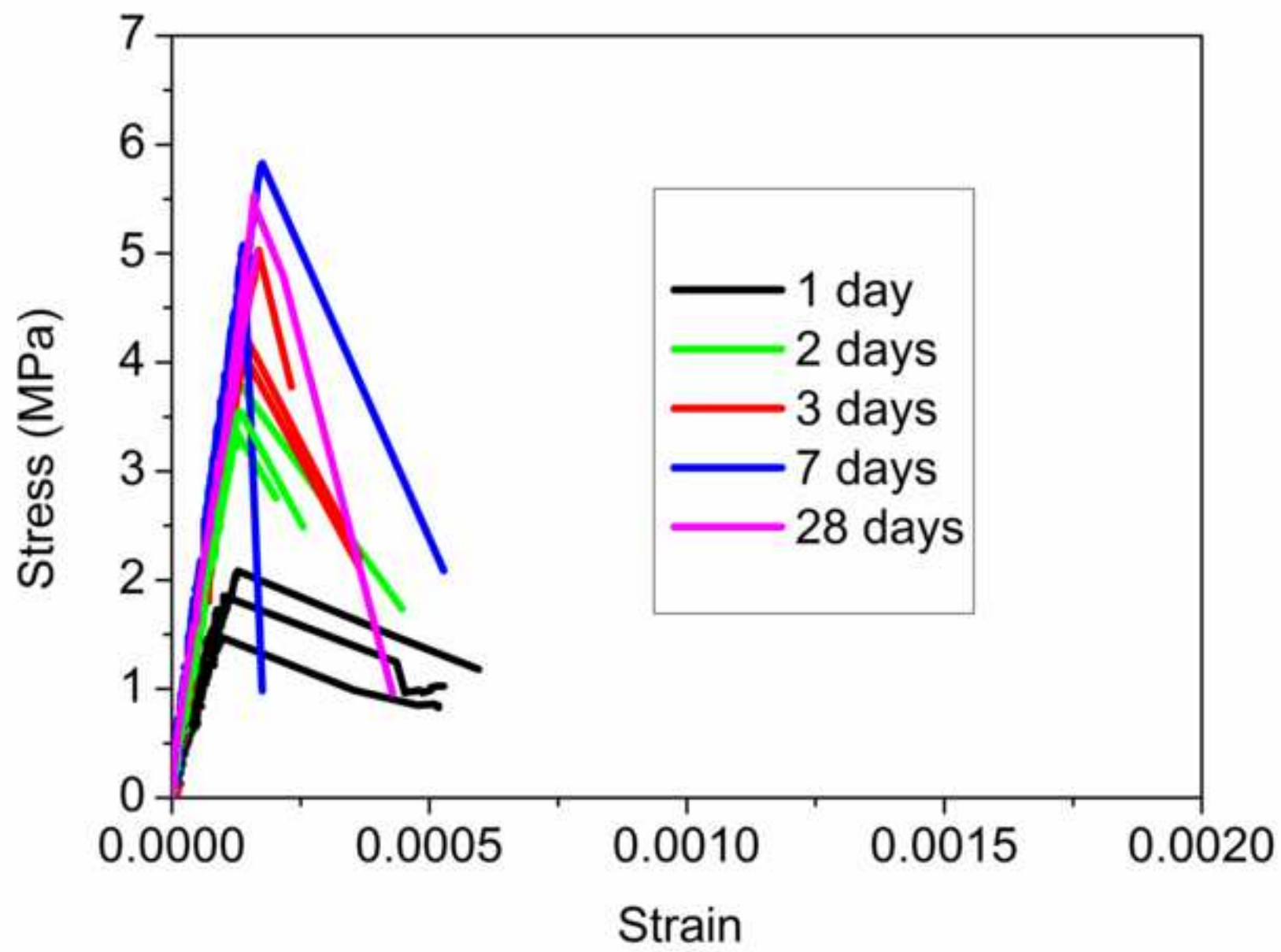


Fig. 4c
[Click here to download high resolution image](#)

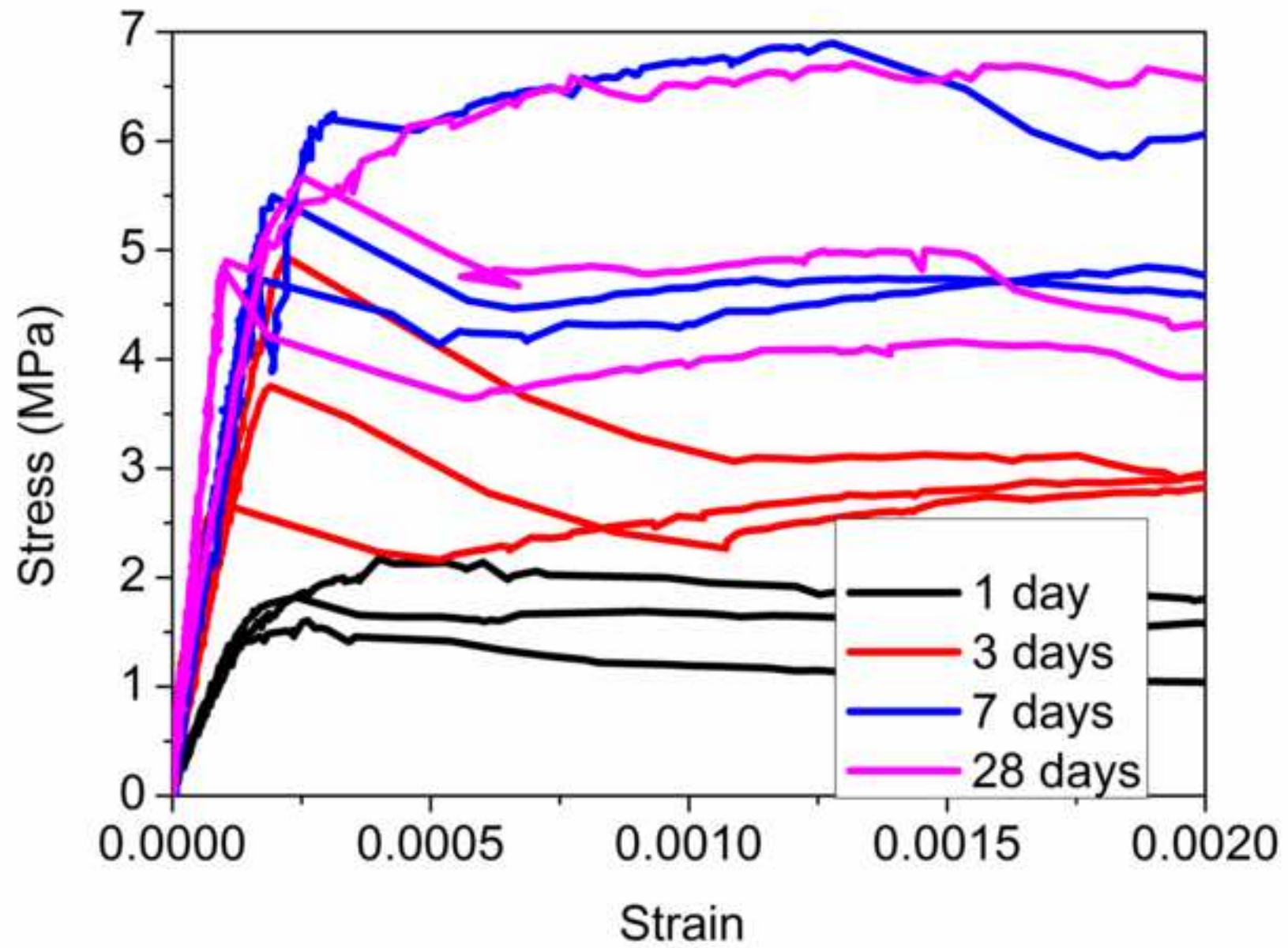


Fig. 5

[Click here to download high resolution image](#)

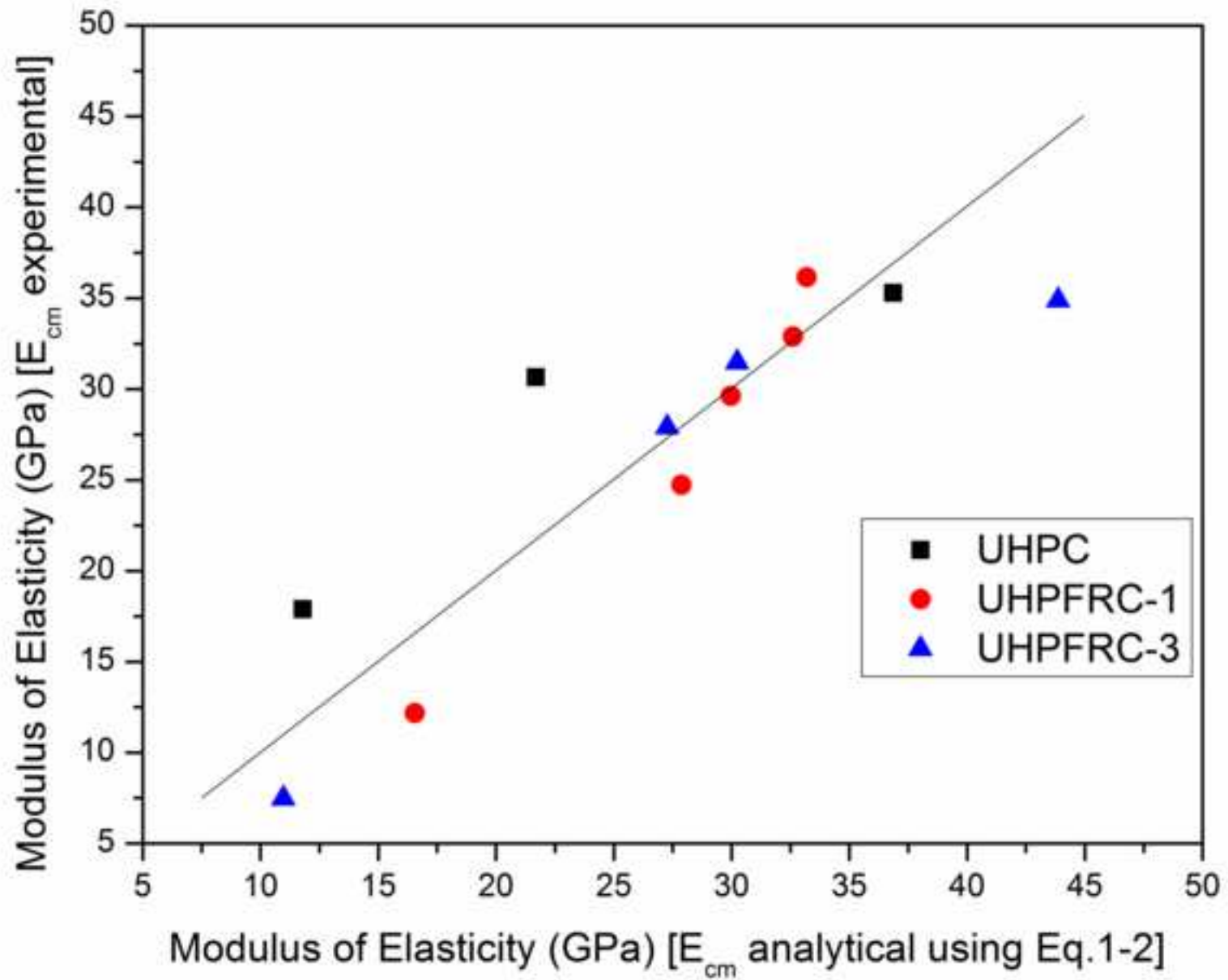


Fig. 6

[Click here to download high resolution image](#)

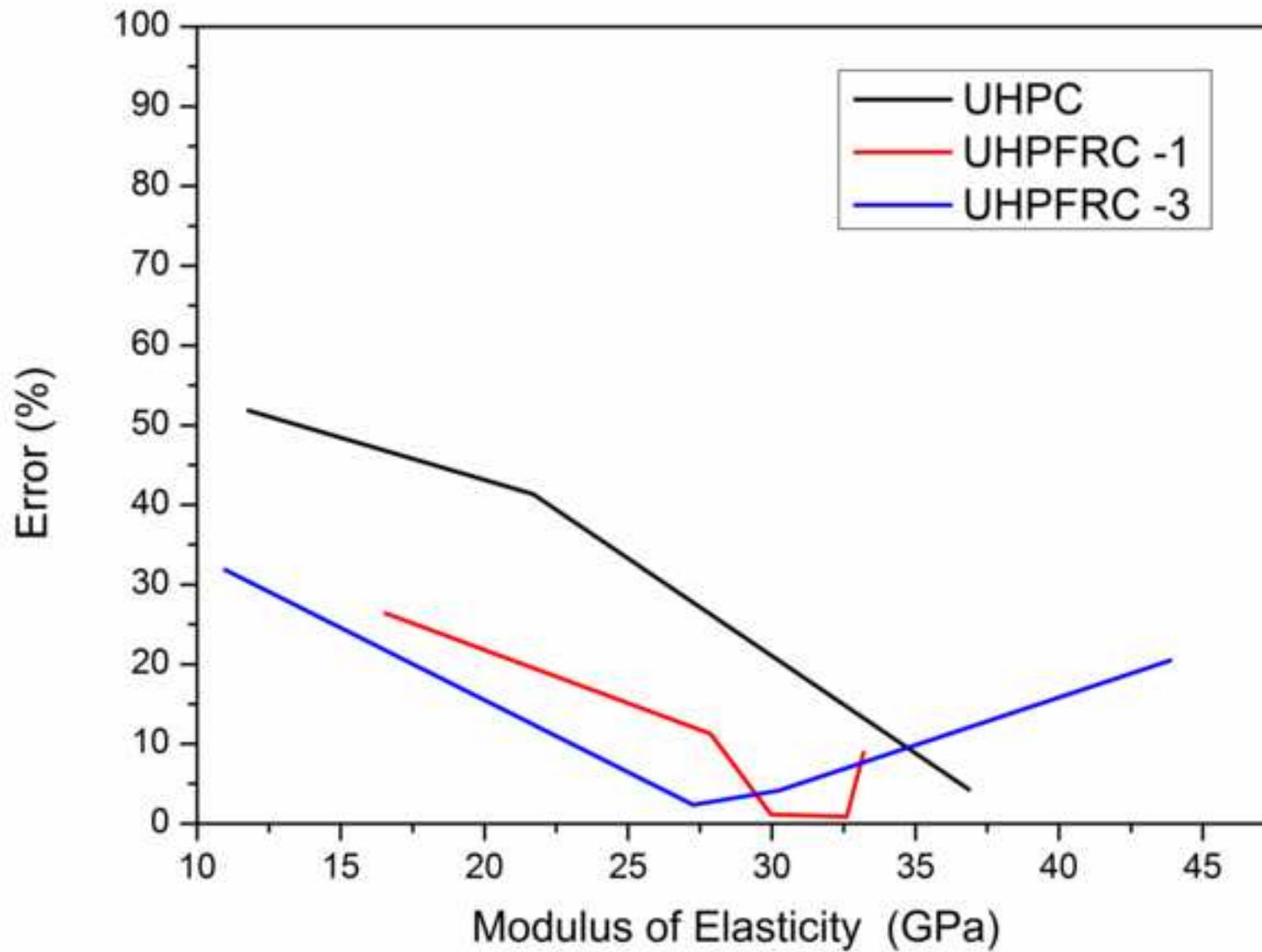


Fig. 7

[Click here to download high resolution image](#)

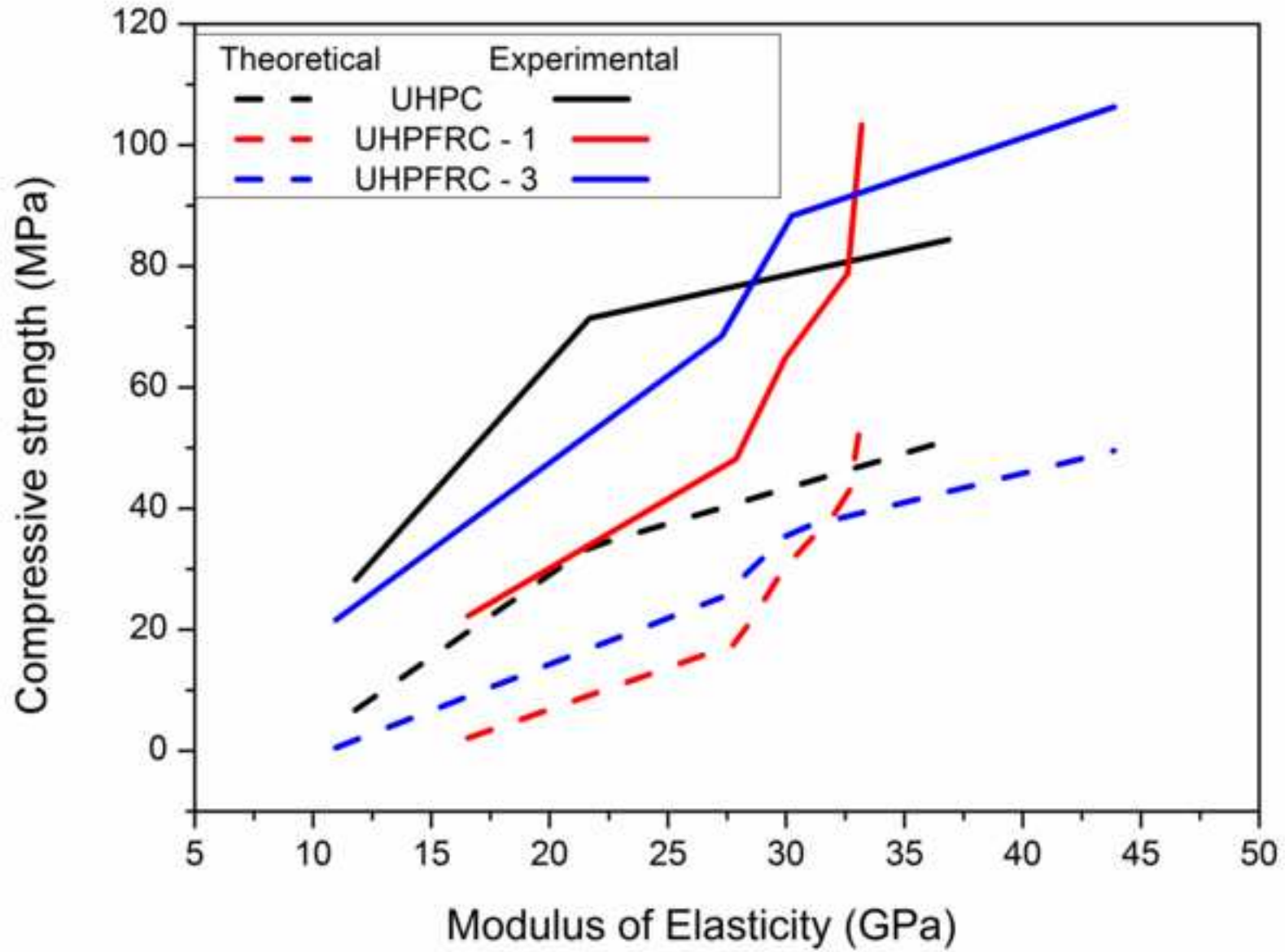


Fig. 8a

[Click here to download high resolution image](#)

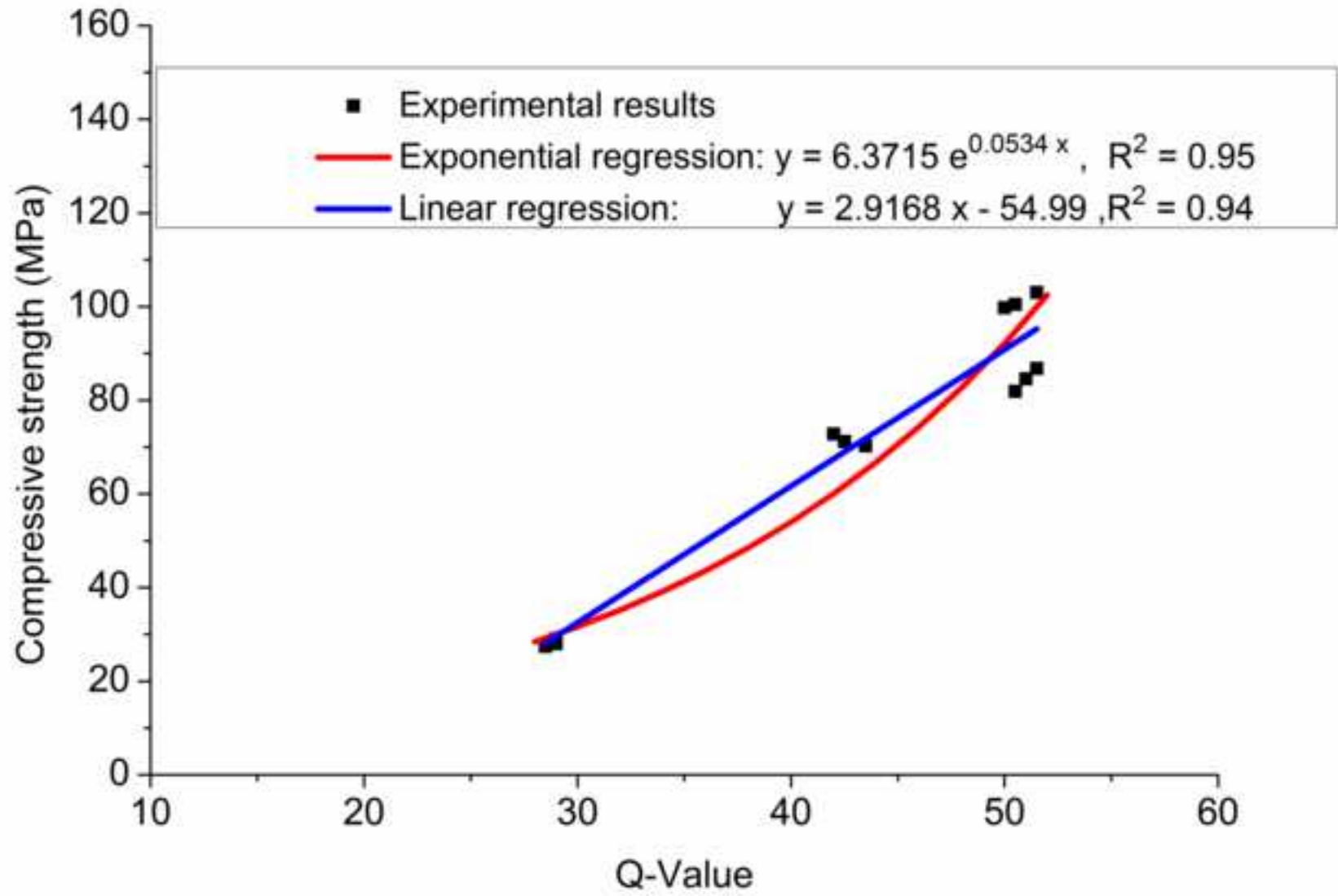


Fig. 8b

[Click here to download high resolution image](#)

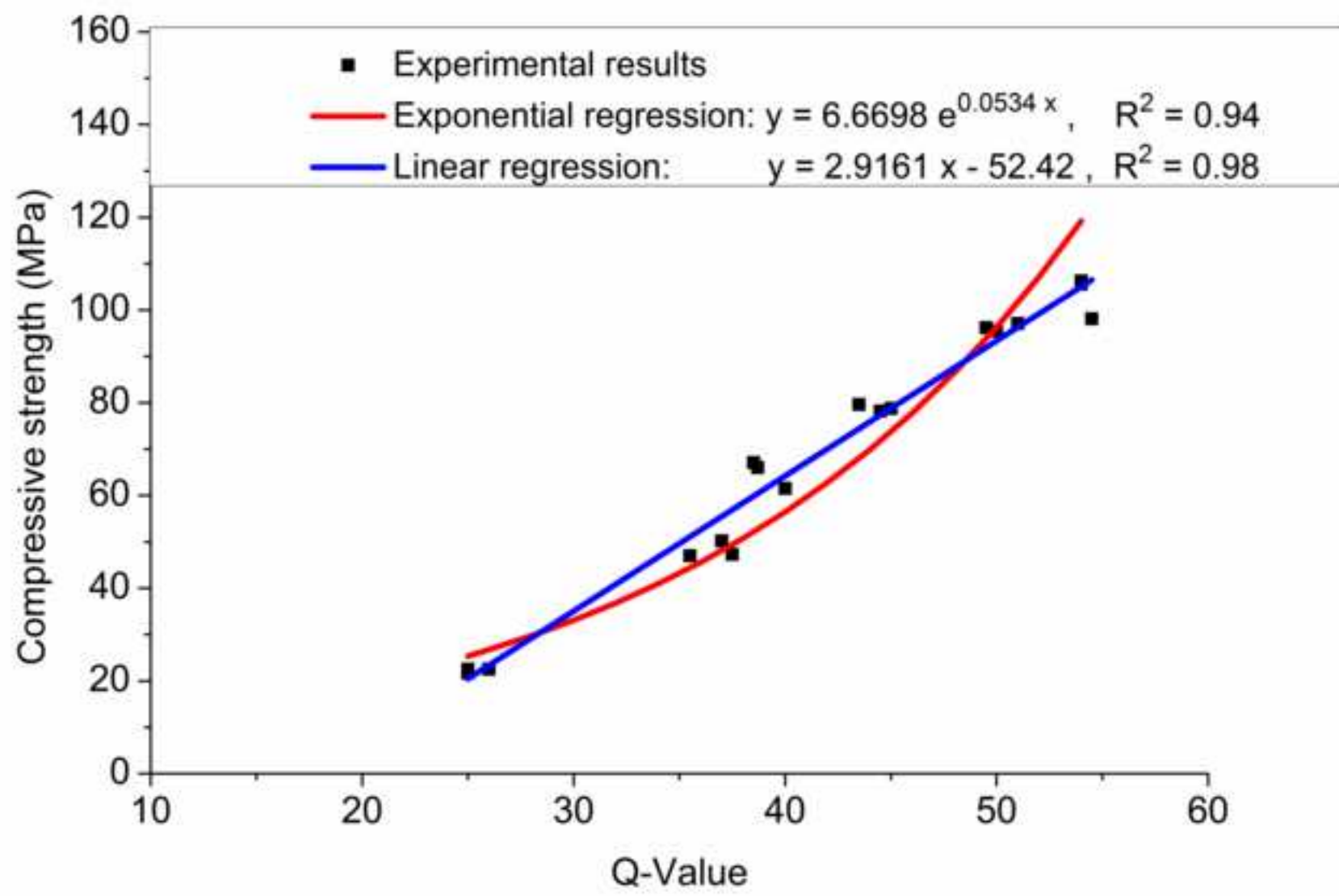


Fig. 8c

[Click here to download high resolution image](#)

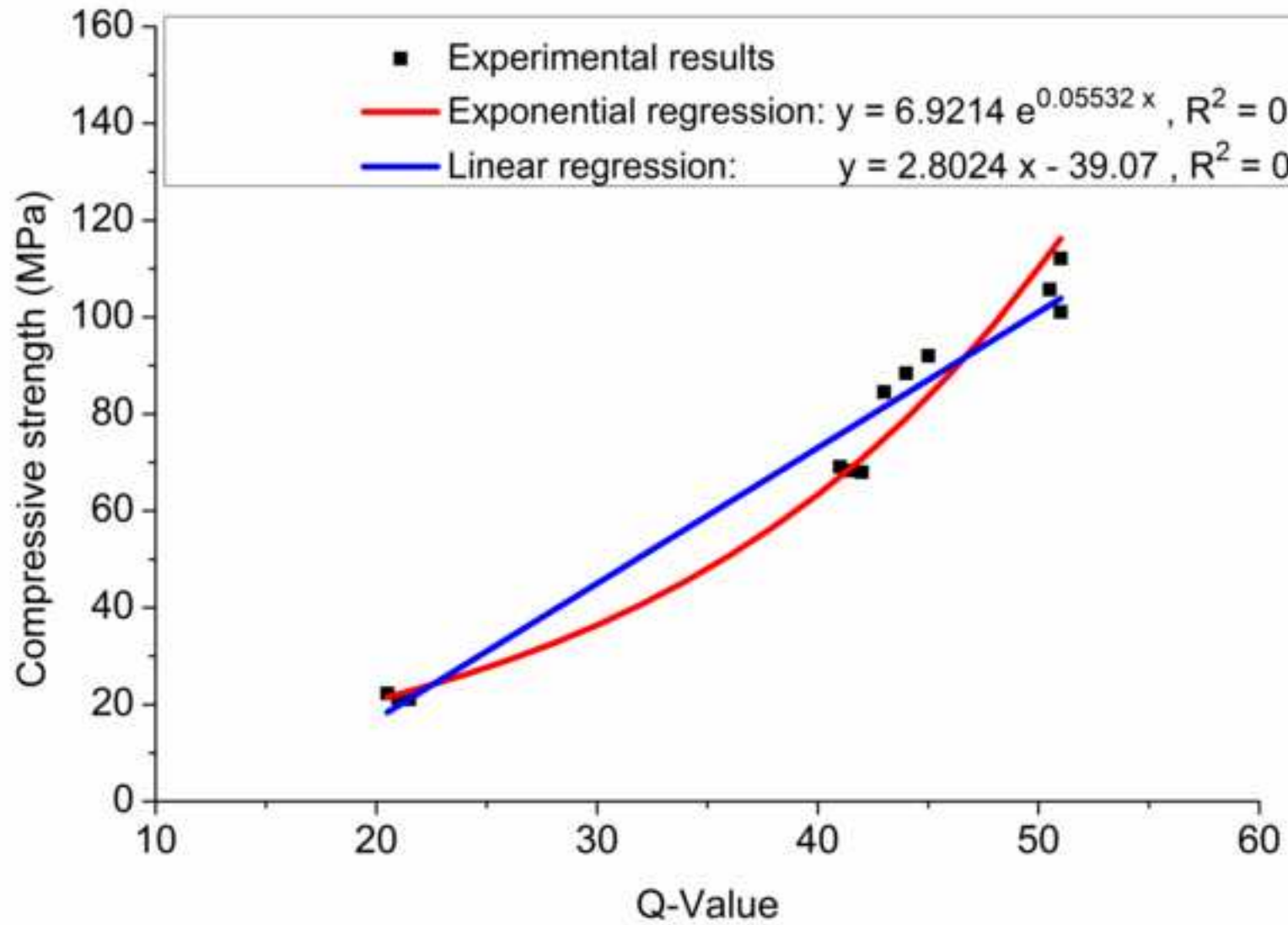


Fig. 9a

[Click here to download high resolution image](#)

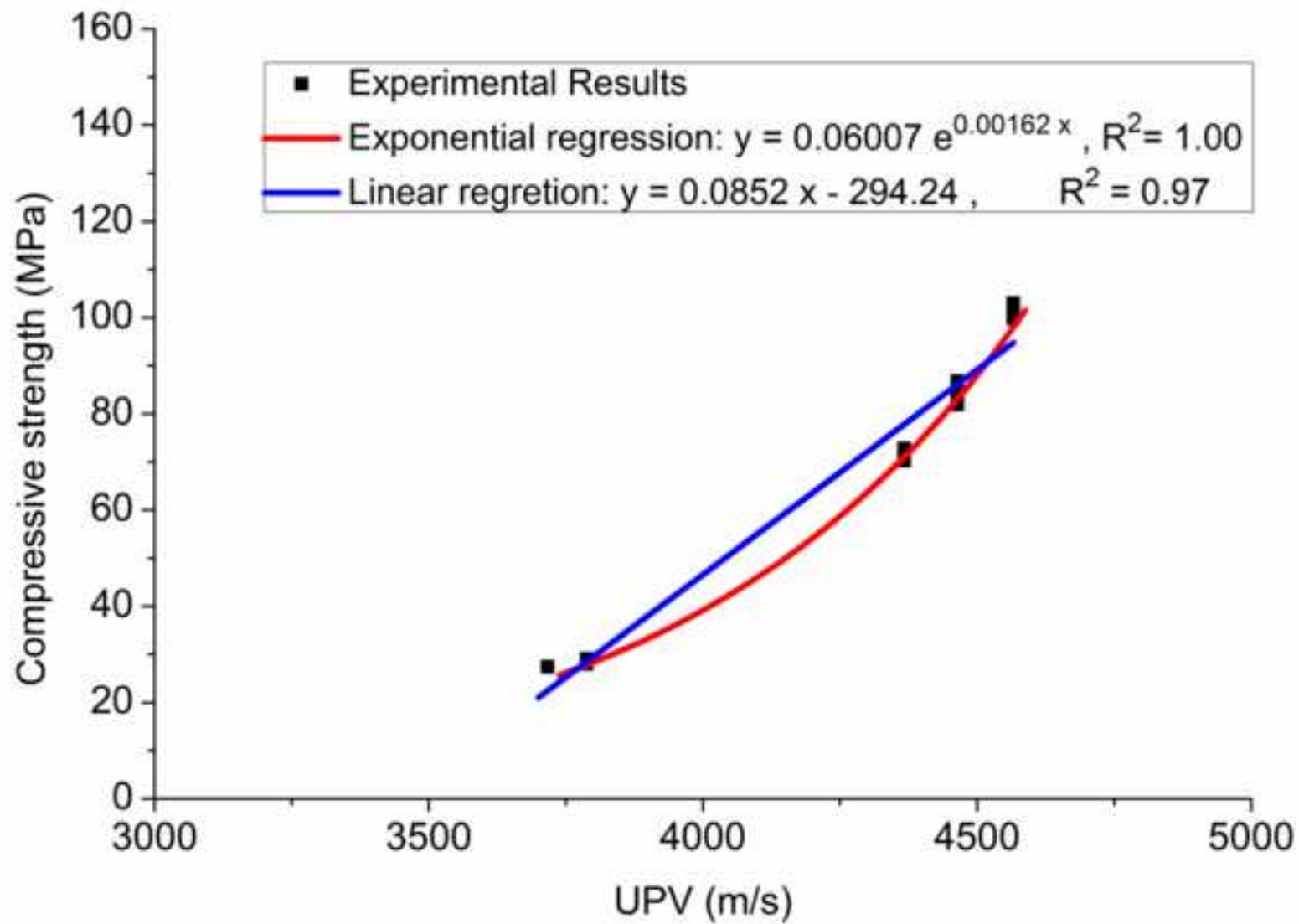


Fig. 9b

[Click here to download high resolution image](#)

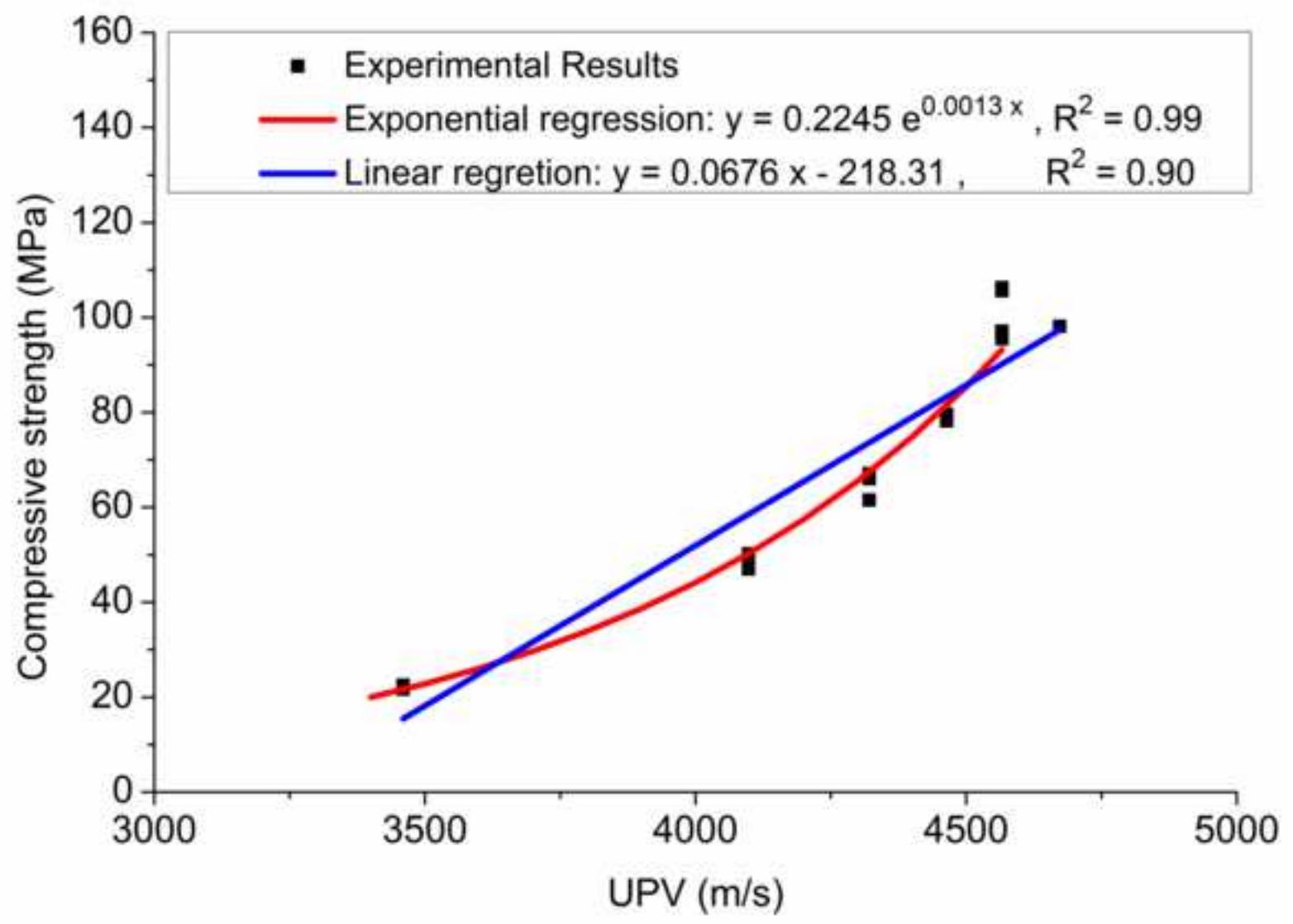


Fig. 9c

[Click here to download high resolution image](#)

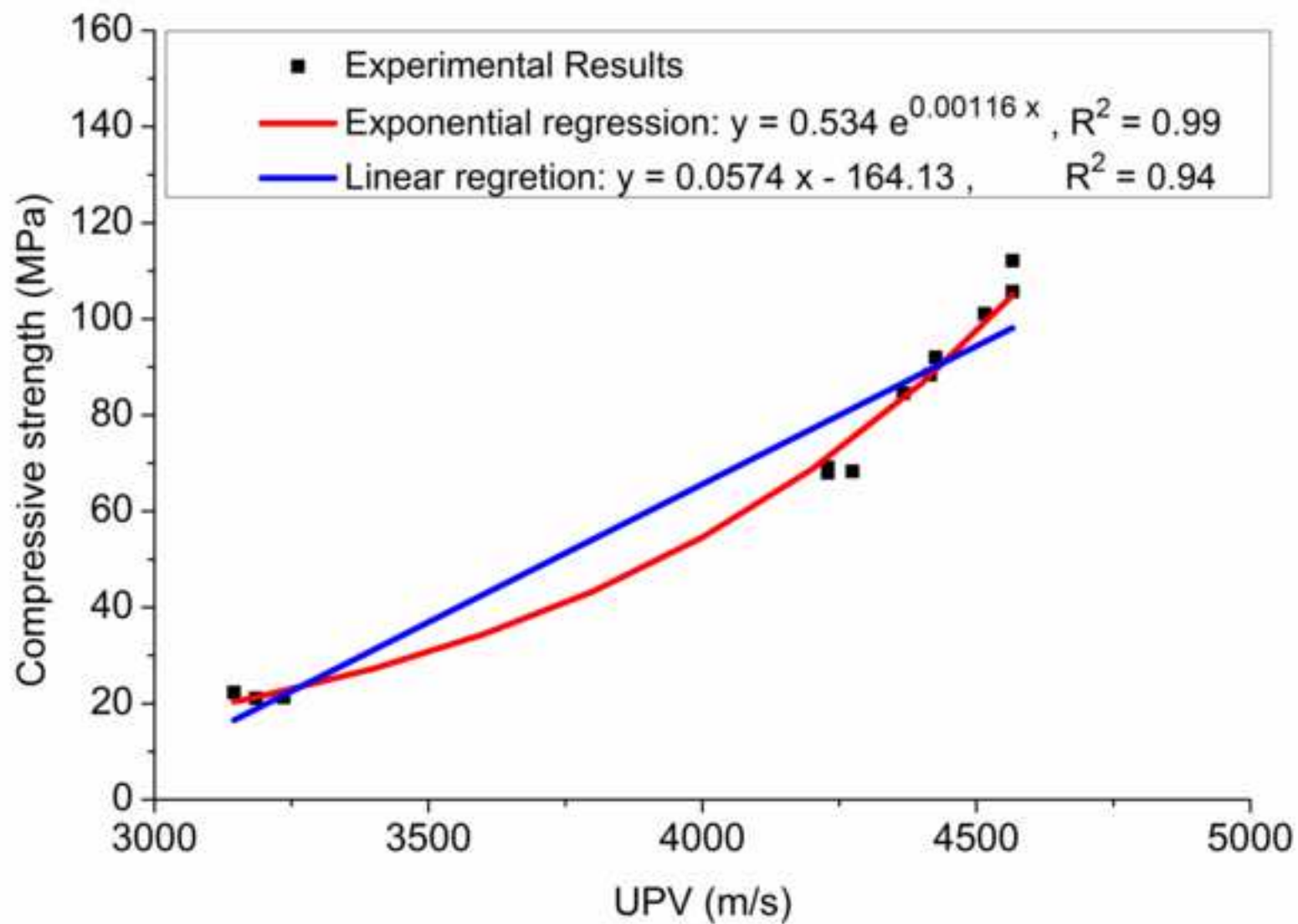


Fig. 10a

[Click here to download high resolution image](#)

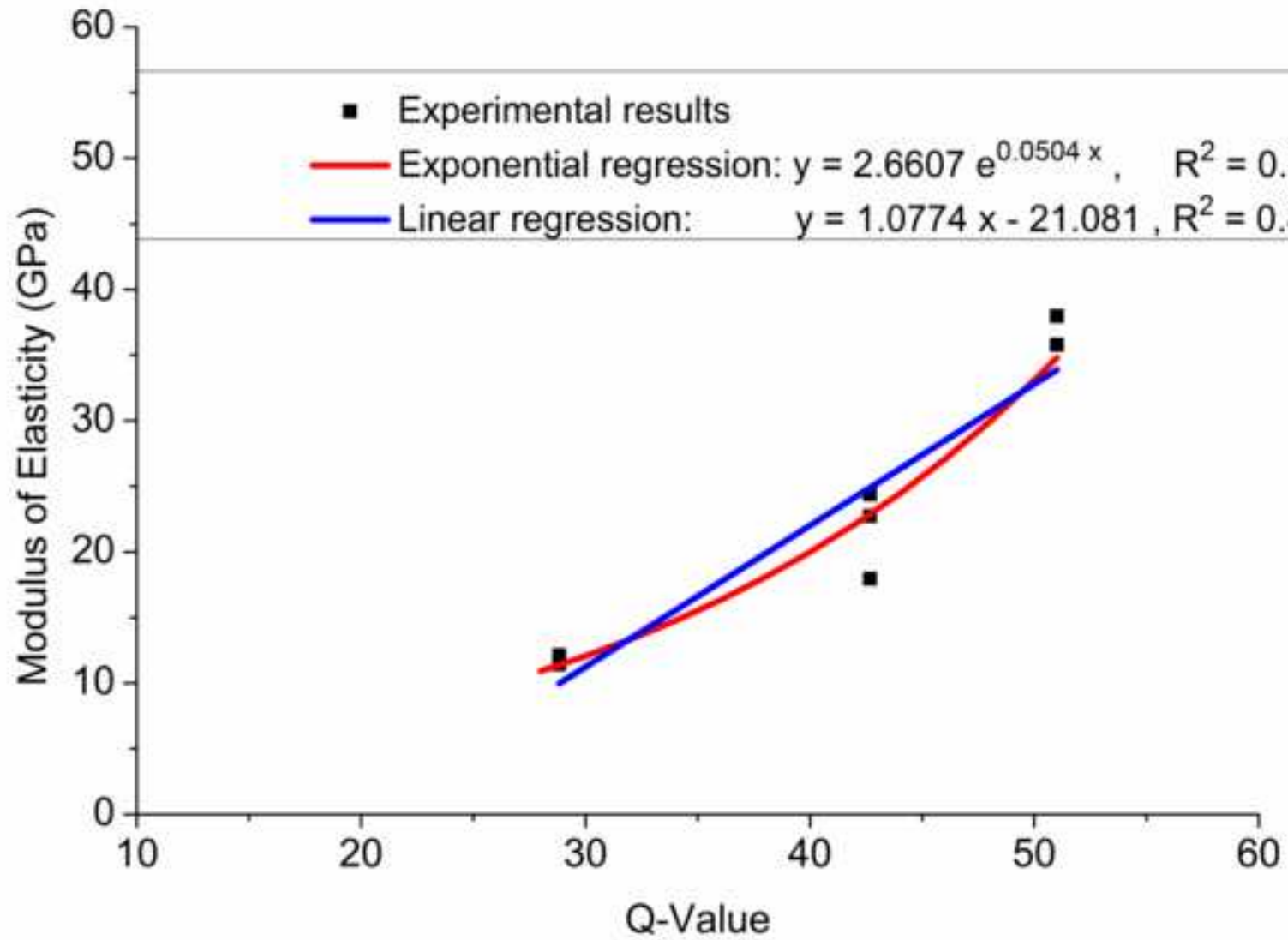


Fig. 10b
[Click here to download high resolution image](#)

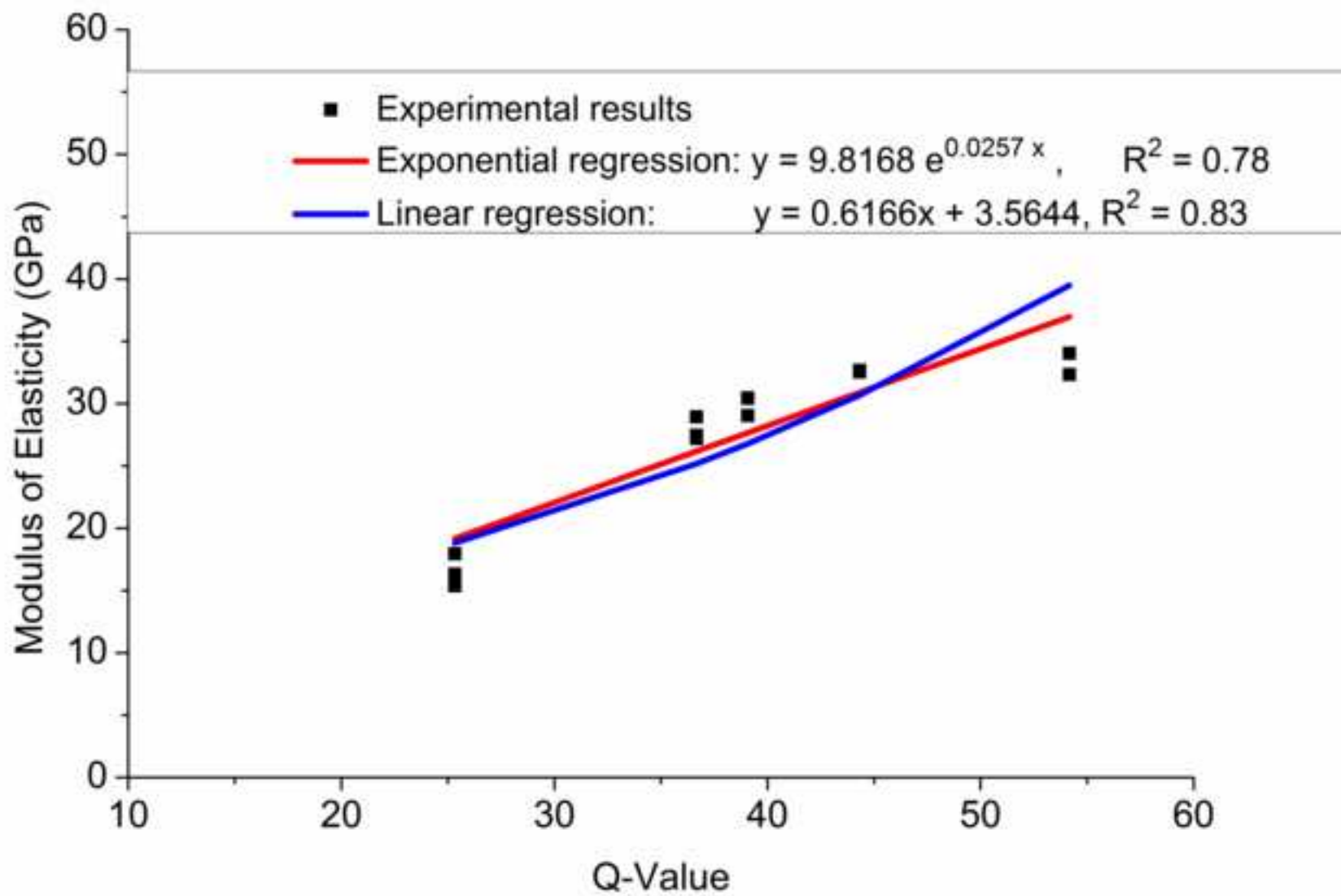


Fig. 10c
[Click here to download high resolution image](#)

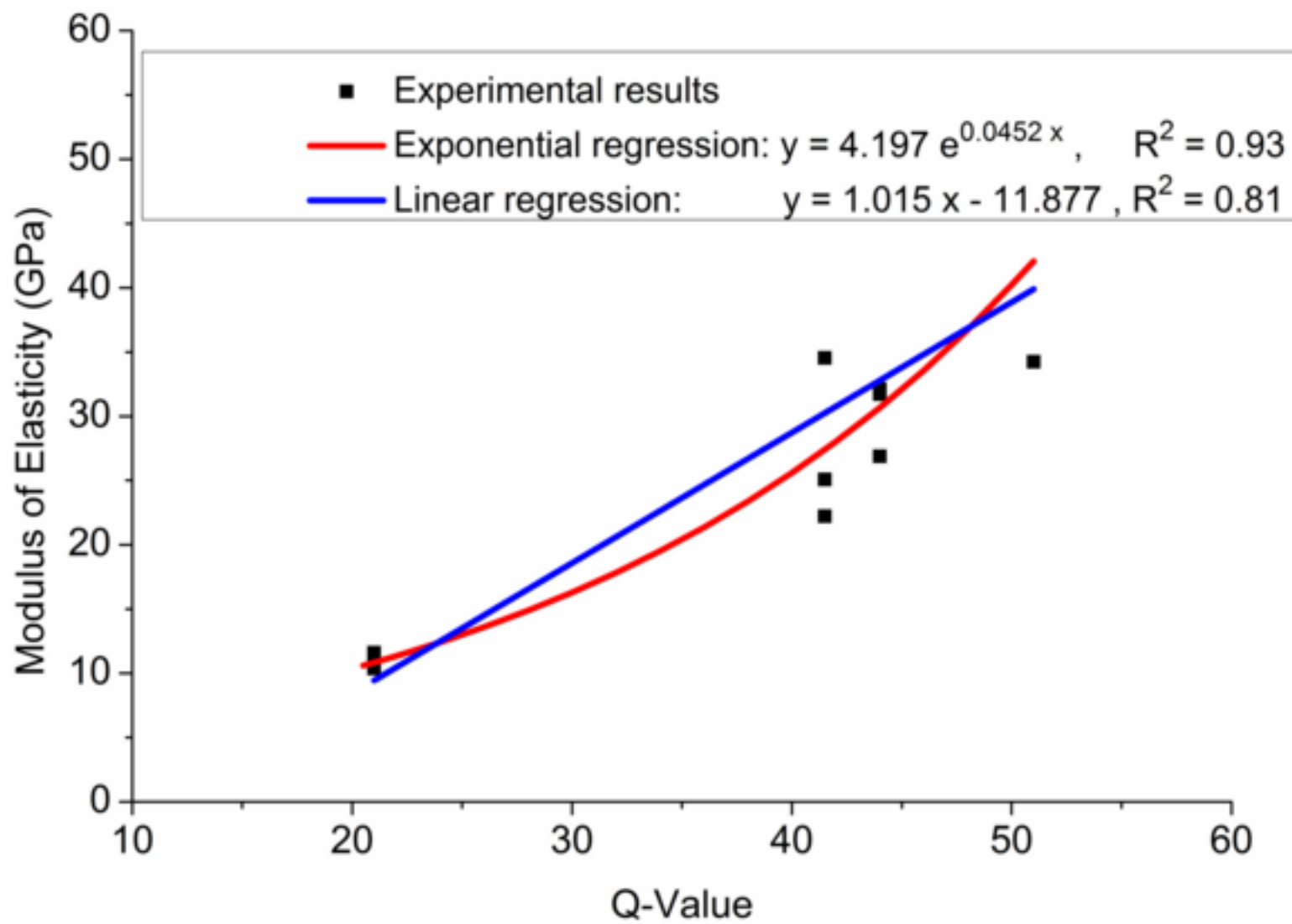


Fig. 11a
[Click here to download high resolution image](#)

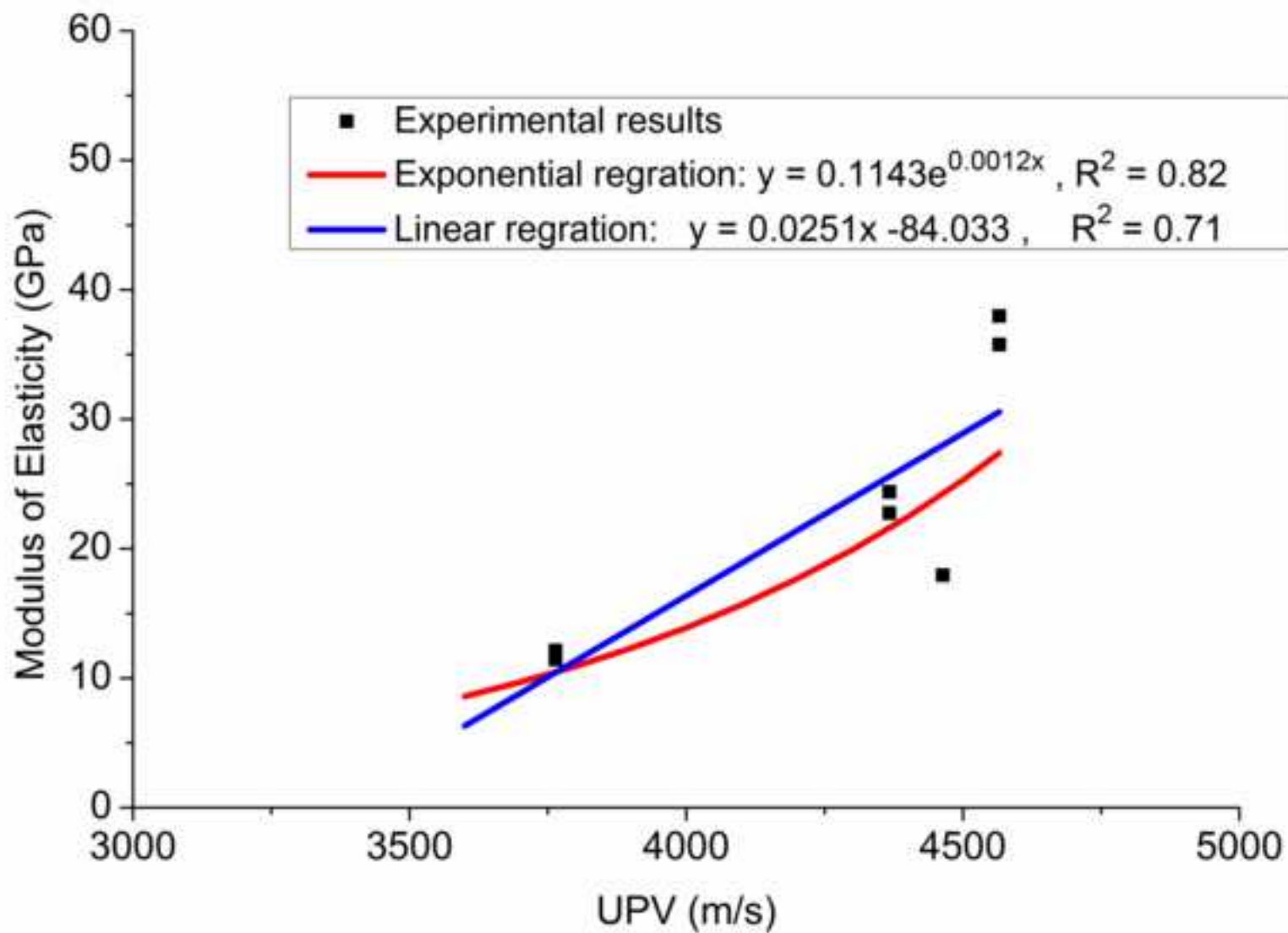


Fig. 11b
[Click here to download high resolution image](#)

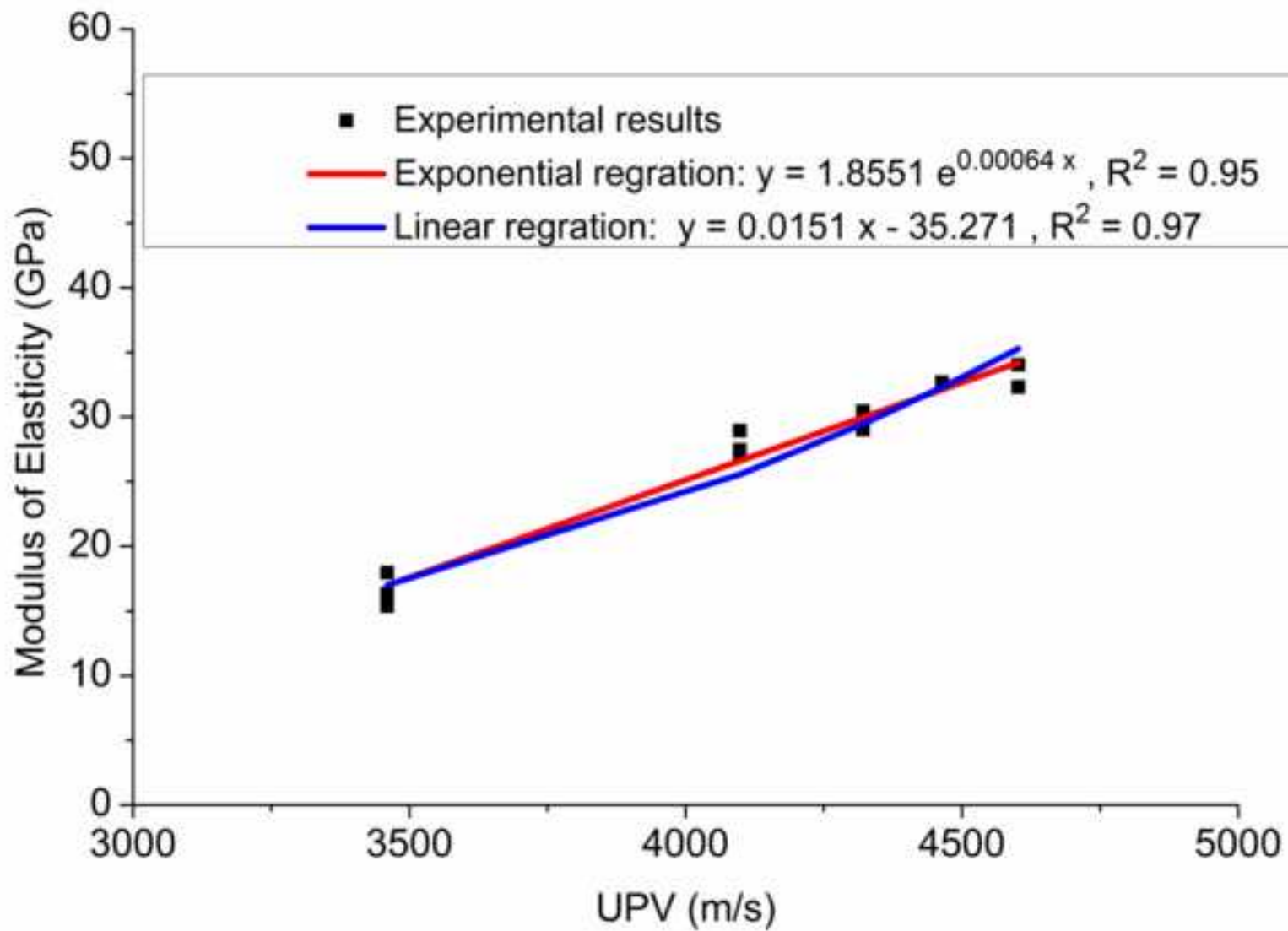


Fig. 11c
[Click here to download high resolution image](#)

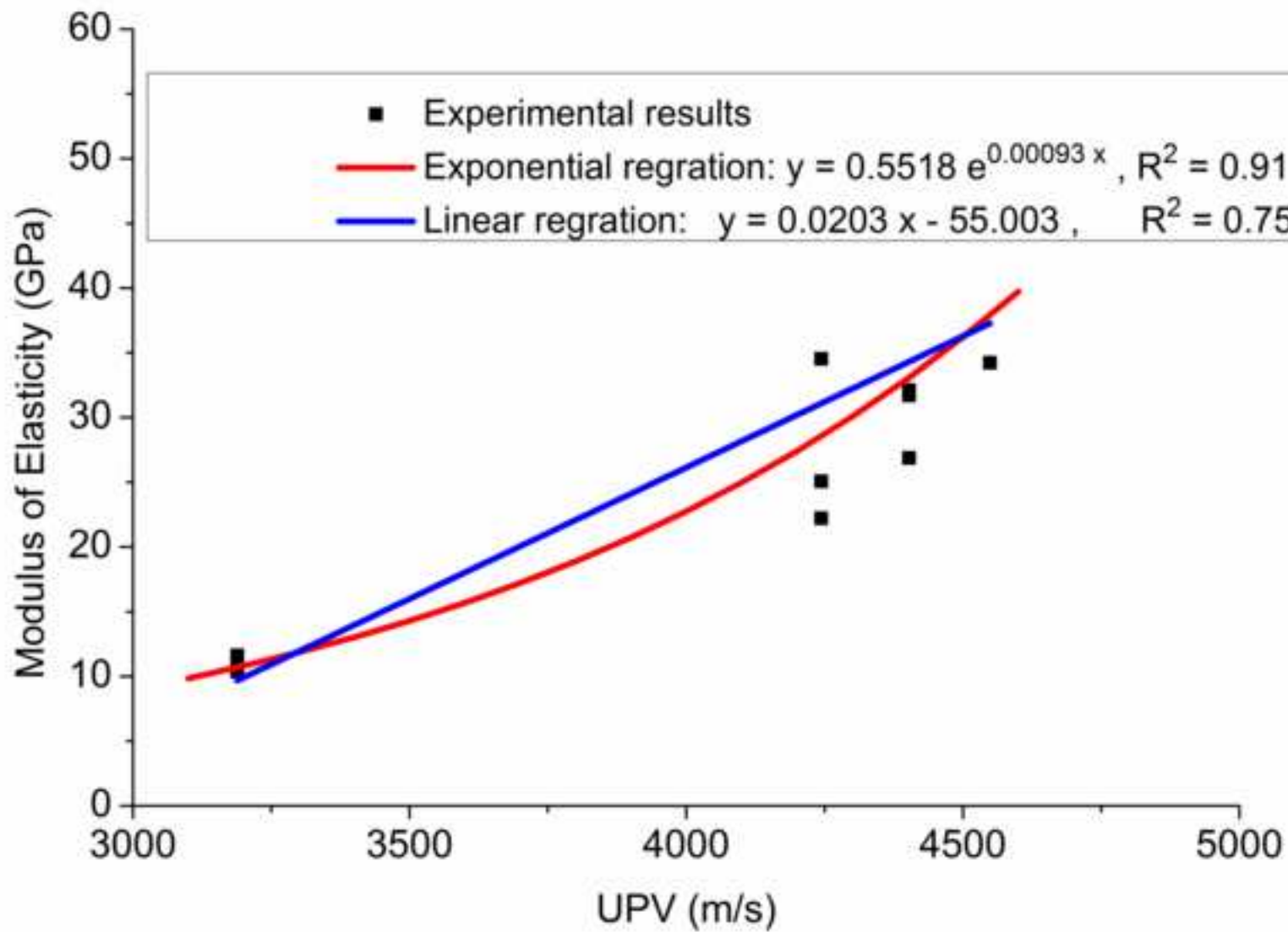


Fig. 12a
[Click here to download high resolution image](#)

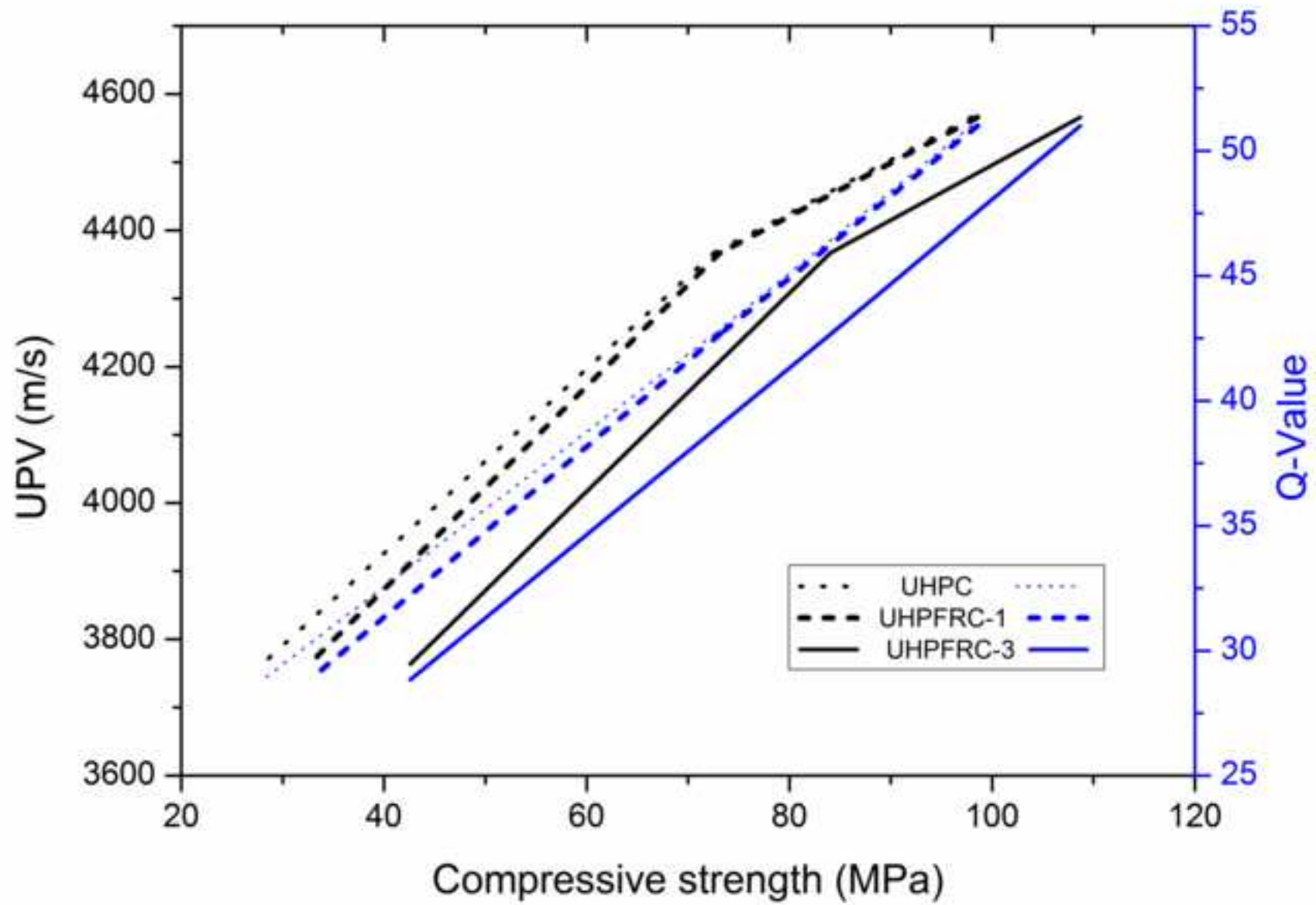


Fig. 12b
[Click here to download high resolution image](#)

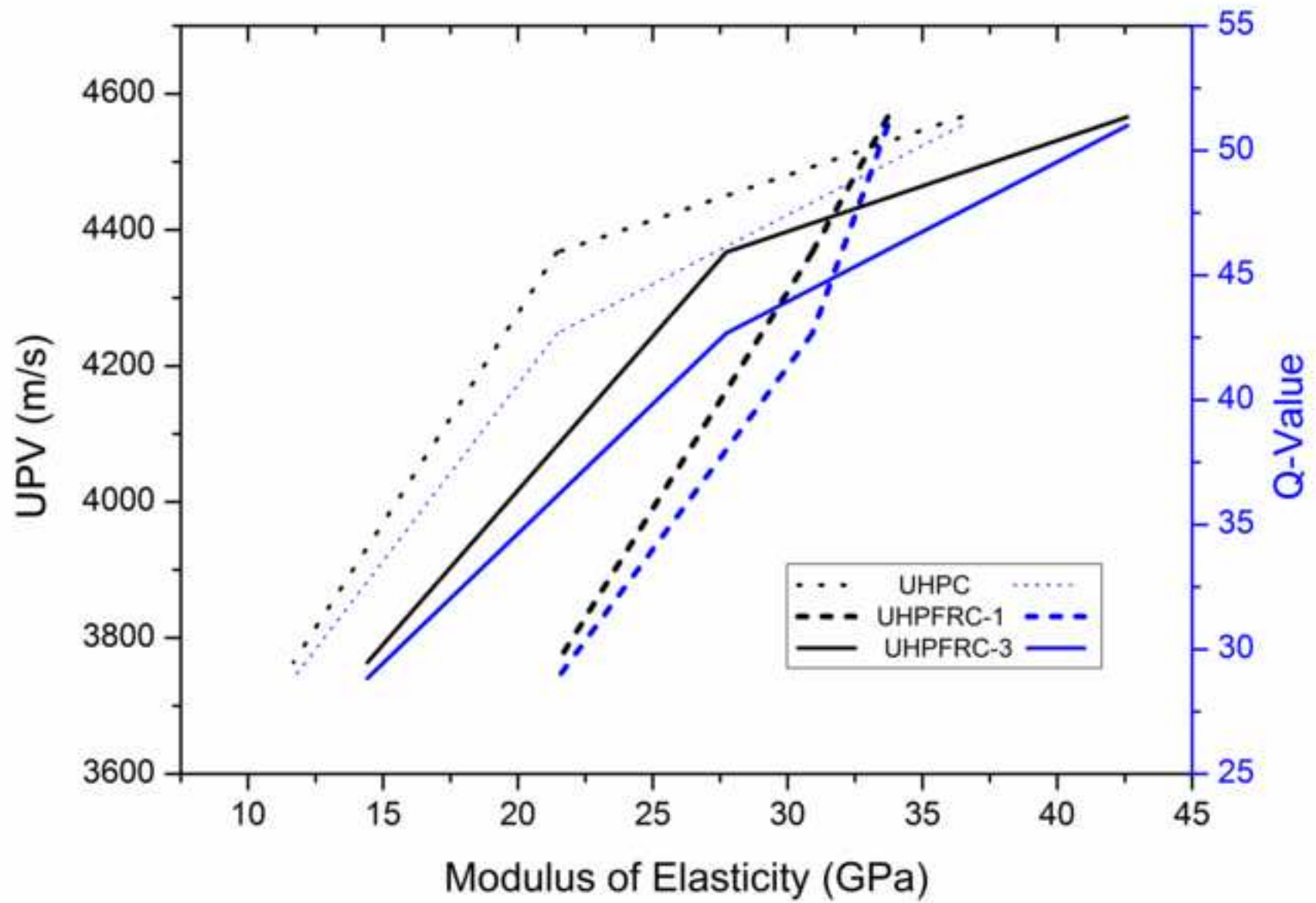


Fig. 13

[Click here to download high resolution image](#)

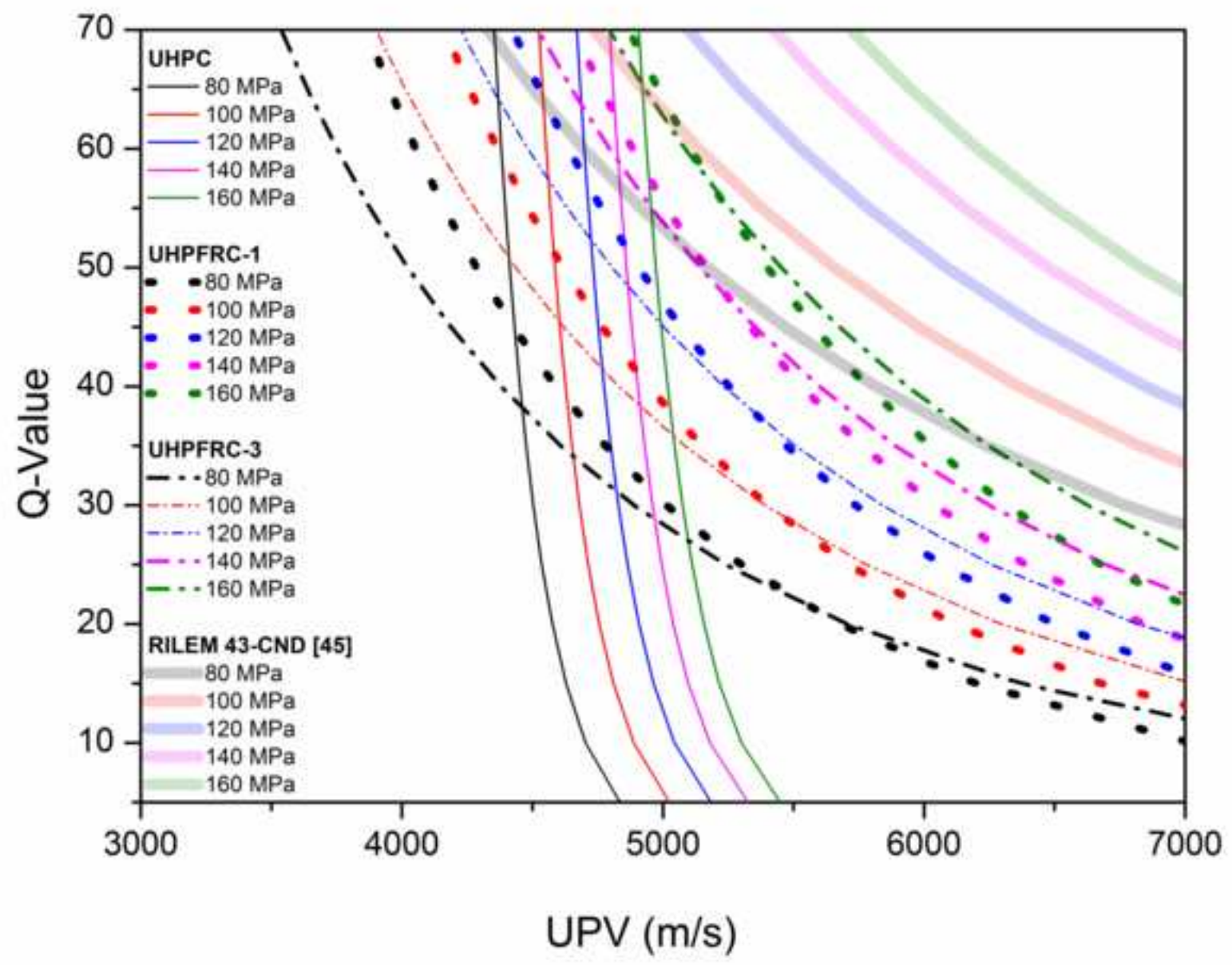


Fig. 14a

[Click here to download high resolution image](#)

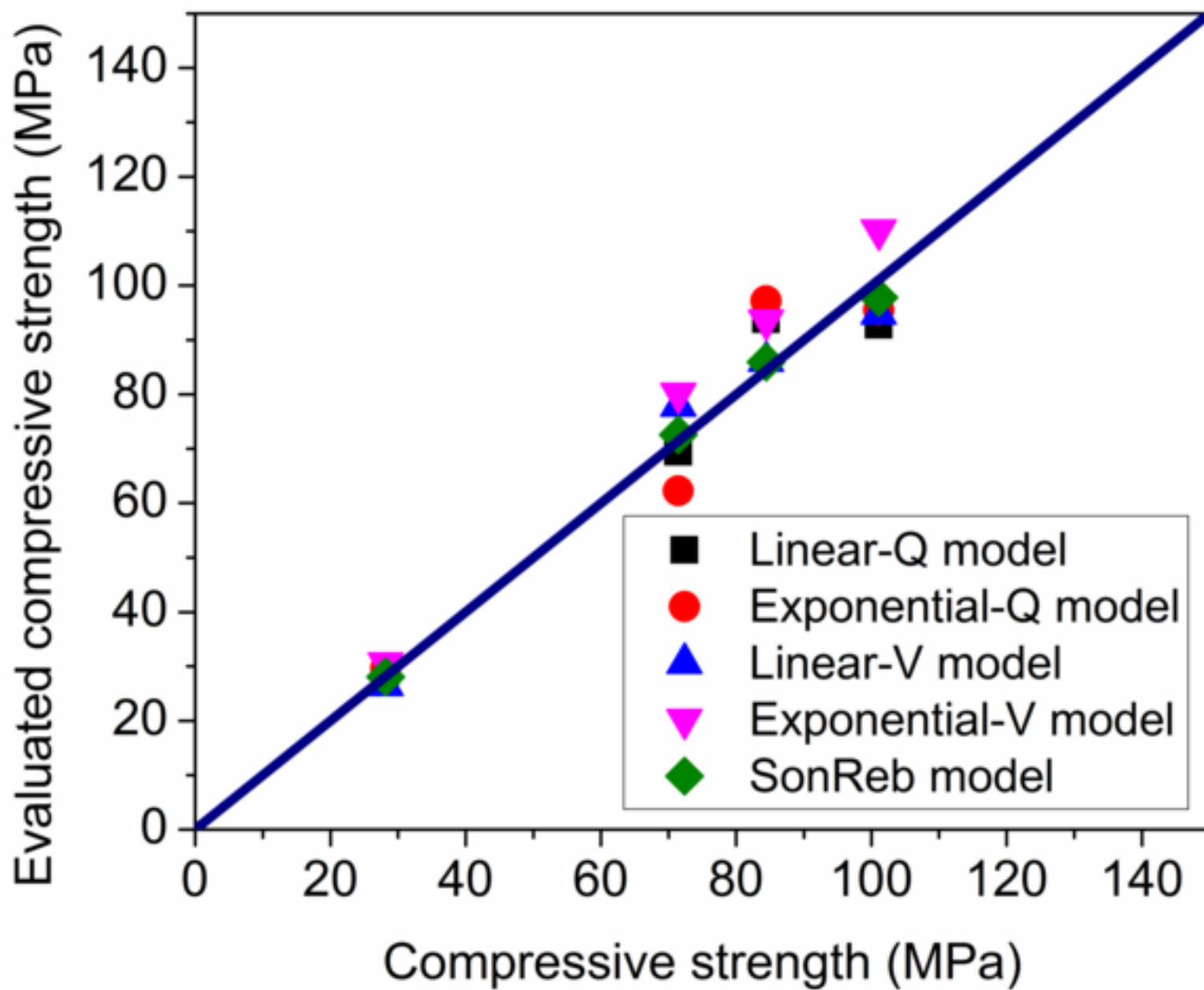


Fig. 14b
[Click here to download high resolution image](#)

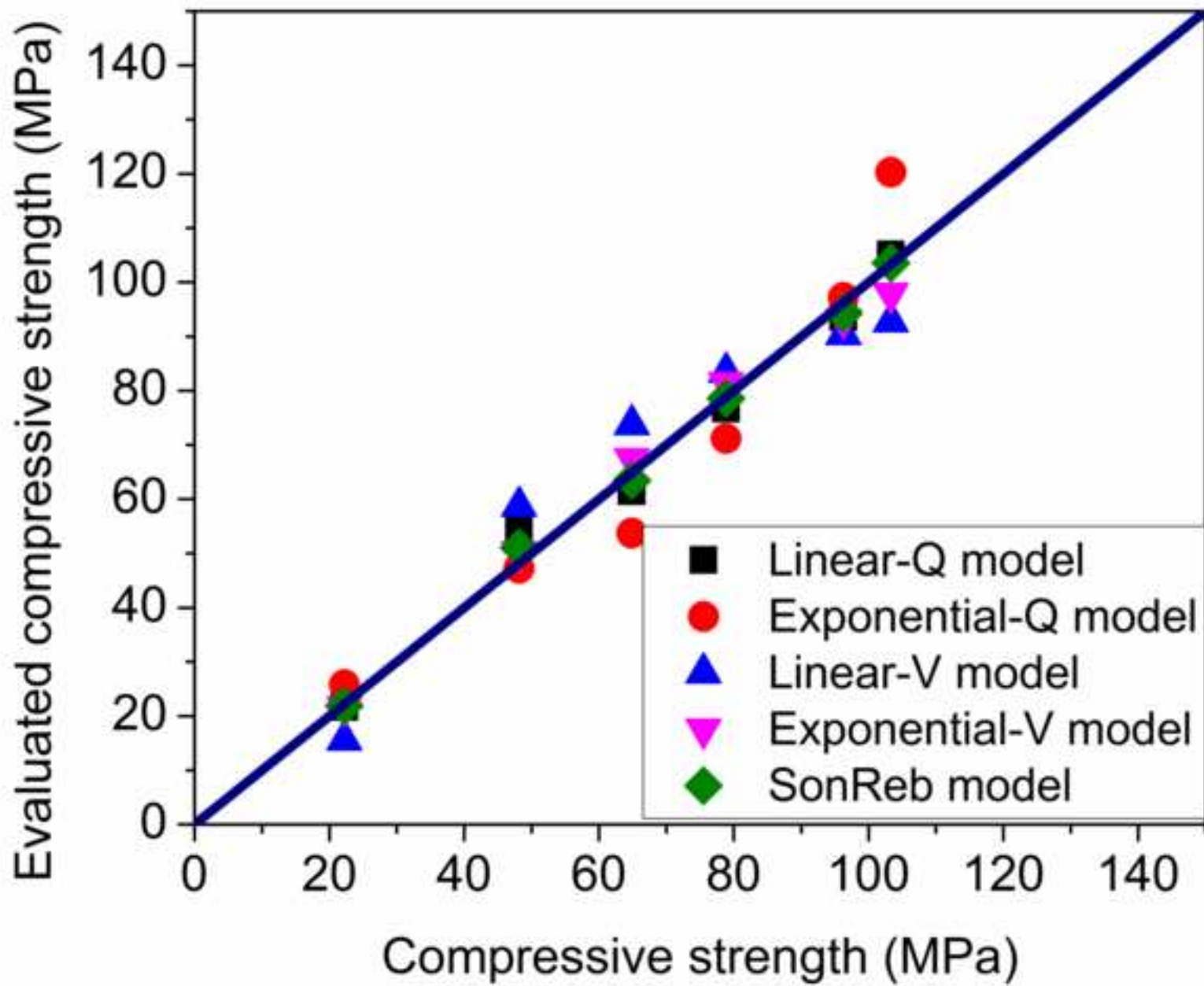


Fig. 14c
[Click here to download high resolution image](#)

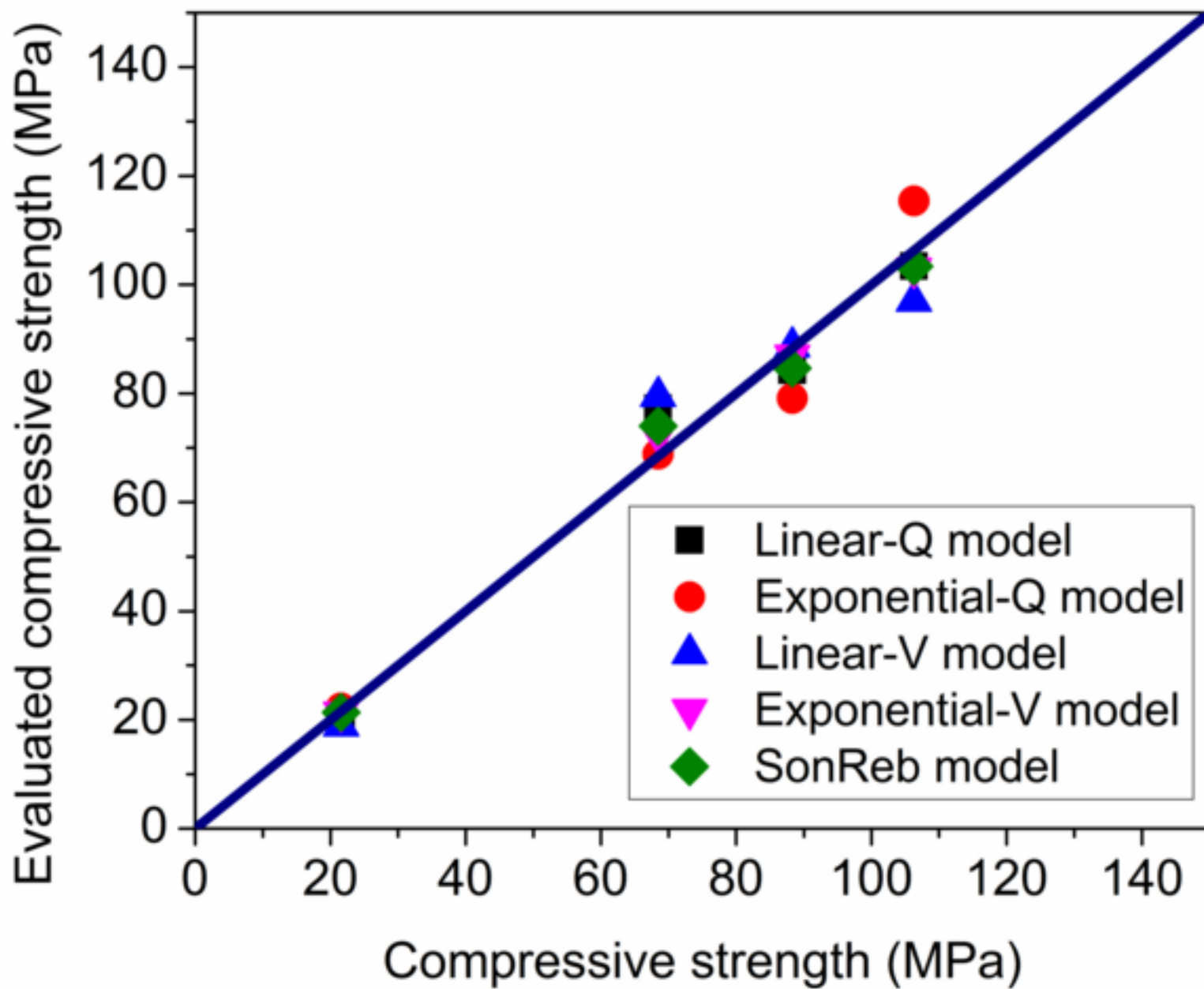


Fig. 15a
[Click here to download high resolution image](#)



Fig. 15b
[Click here to download high resolution image](#)

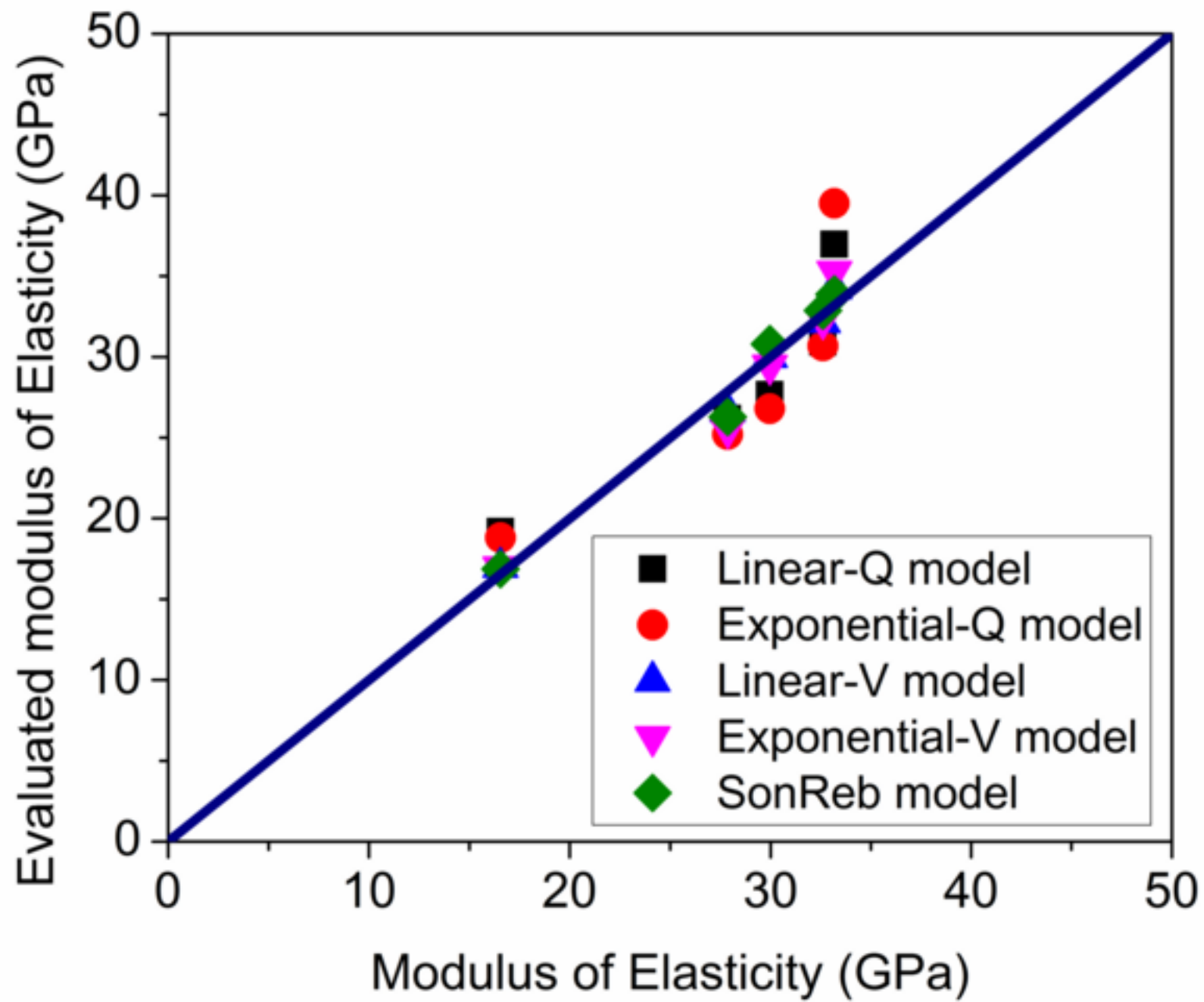


Fig. 15c
[Click here to download high resolution image](#)

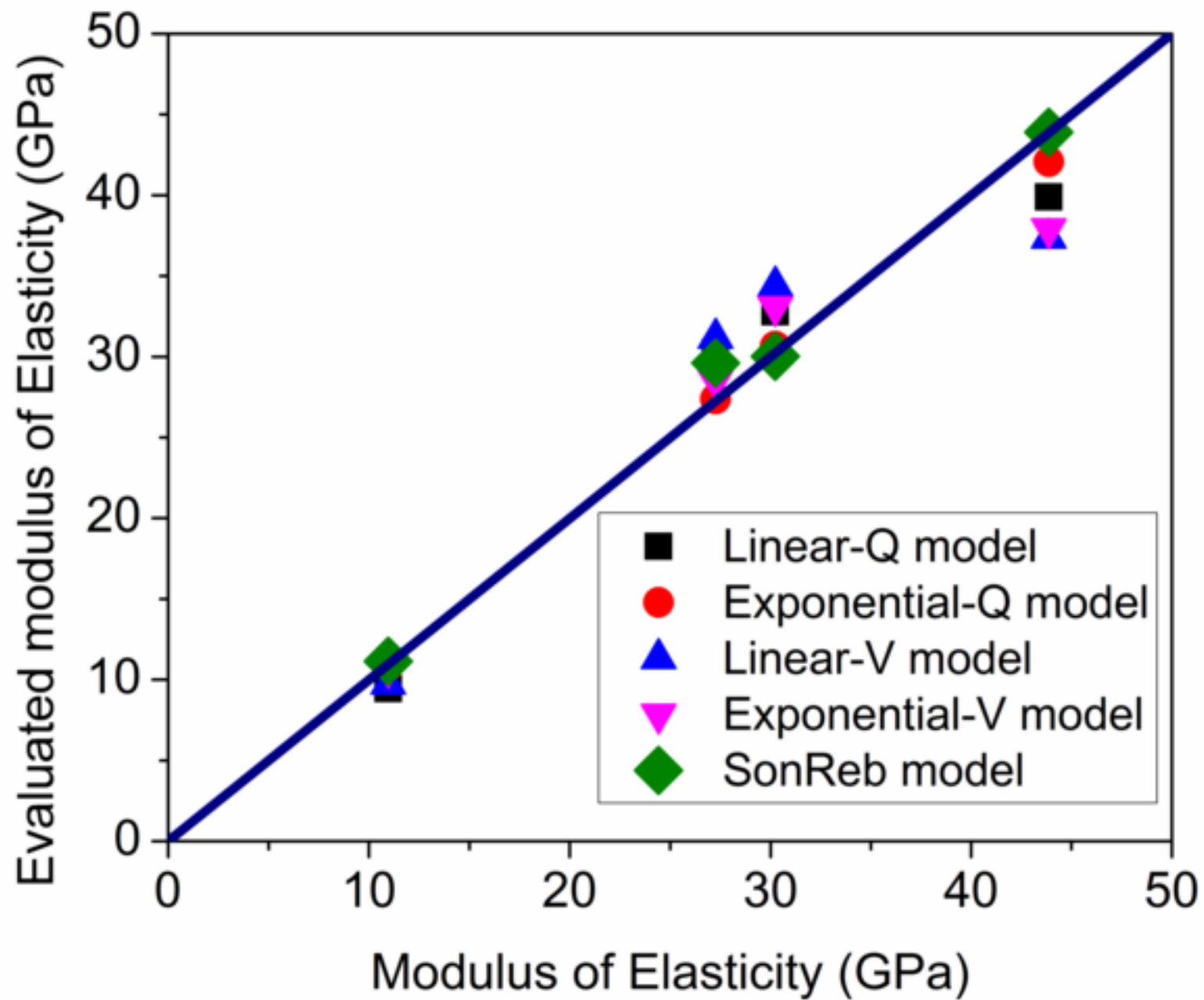


Fig. 16a

[Click here to download high resolution image](#)

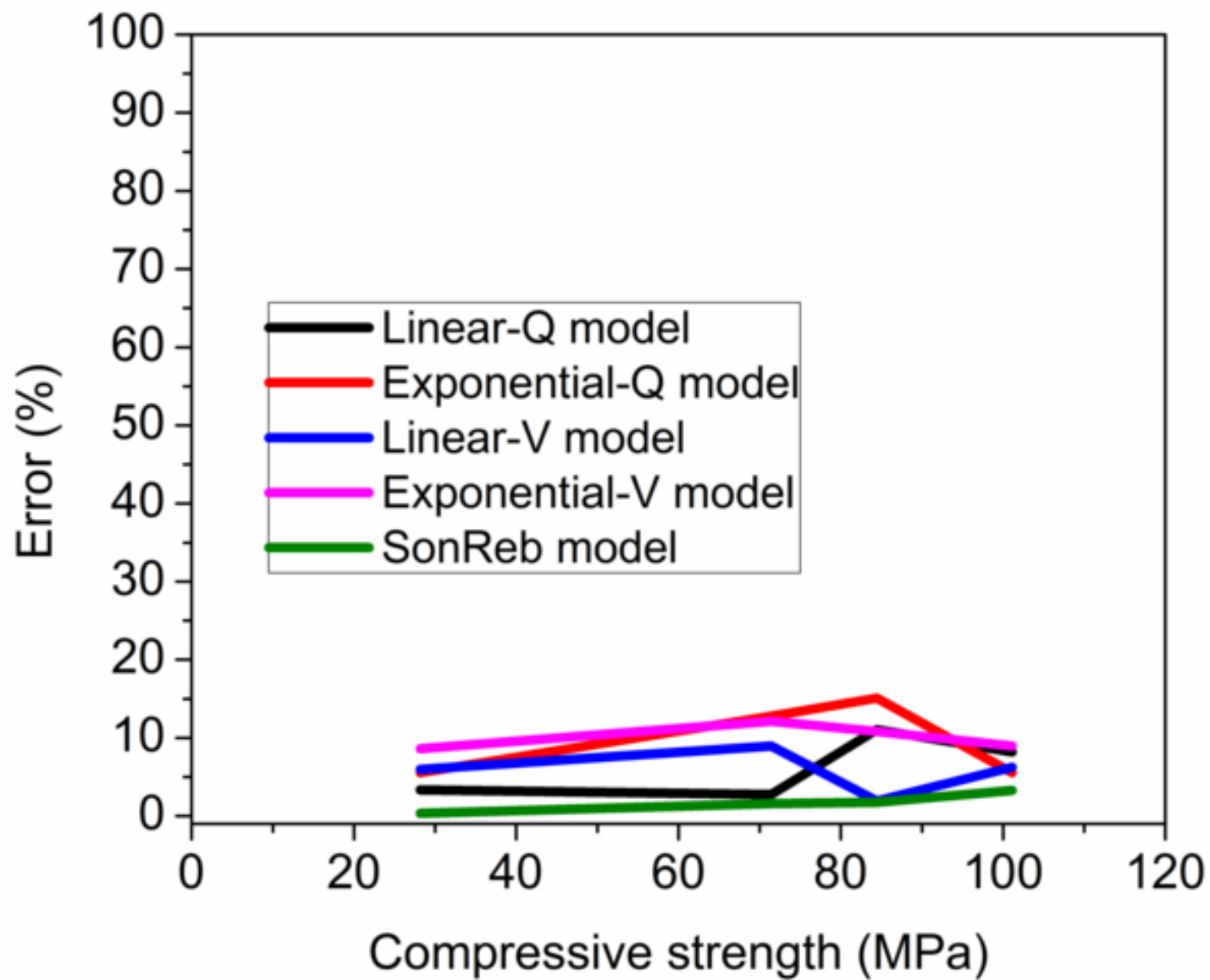


Fig. 16b
[Click here to download high resolution image](#)

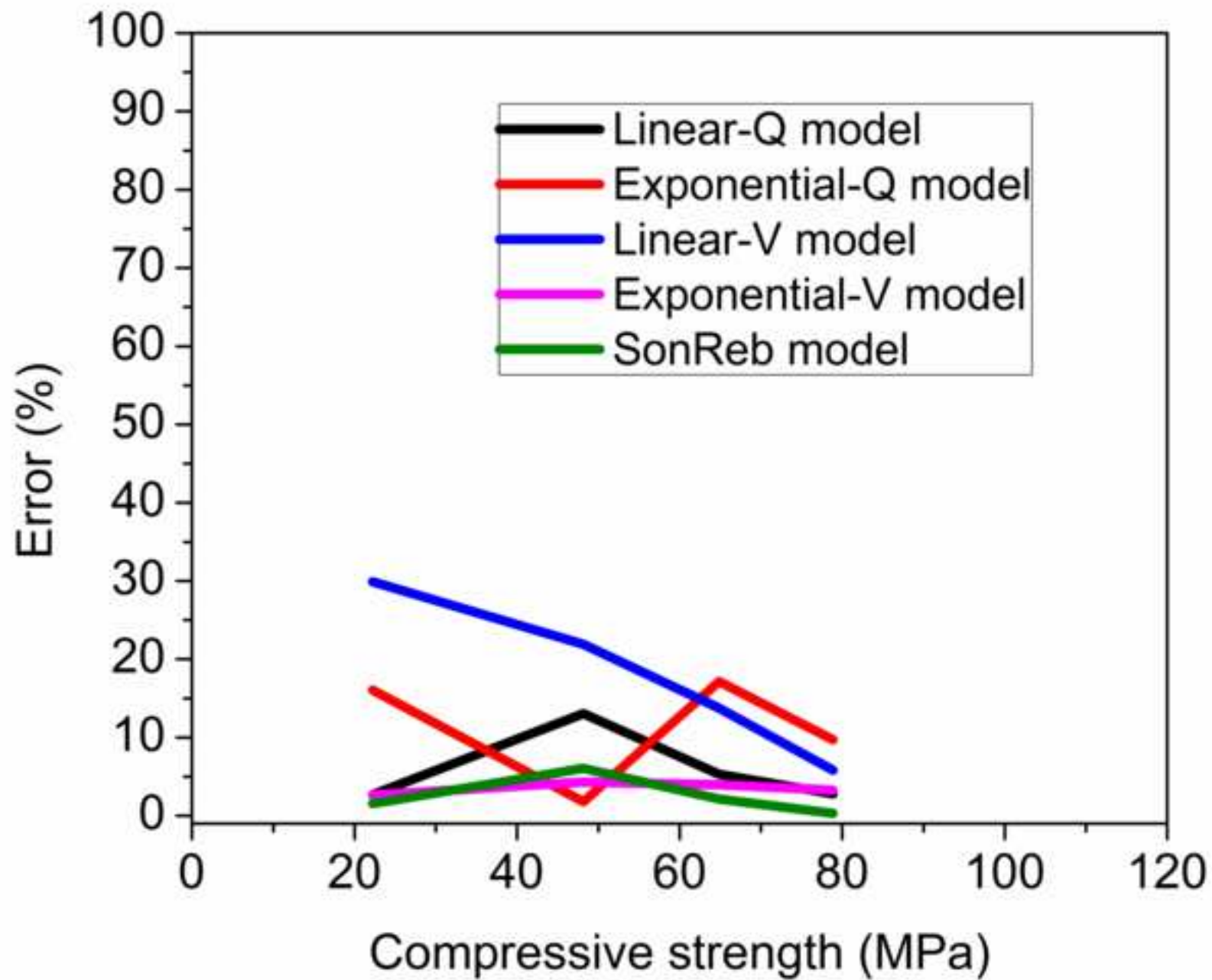


Fig. 16c
[Click here to download high resolution image](#)

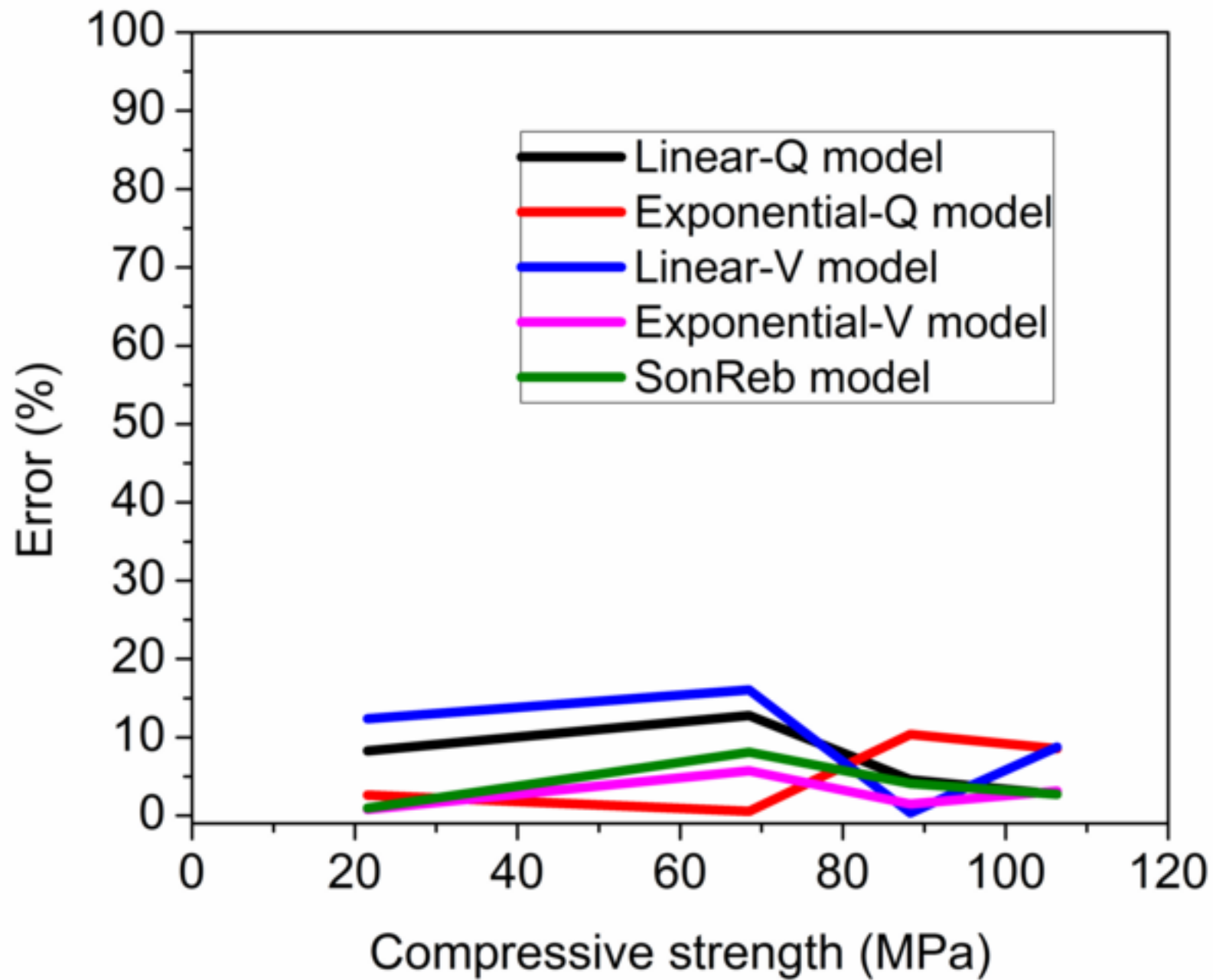


Fig. 17a
[Click here to download high resolution image](#)

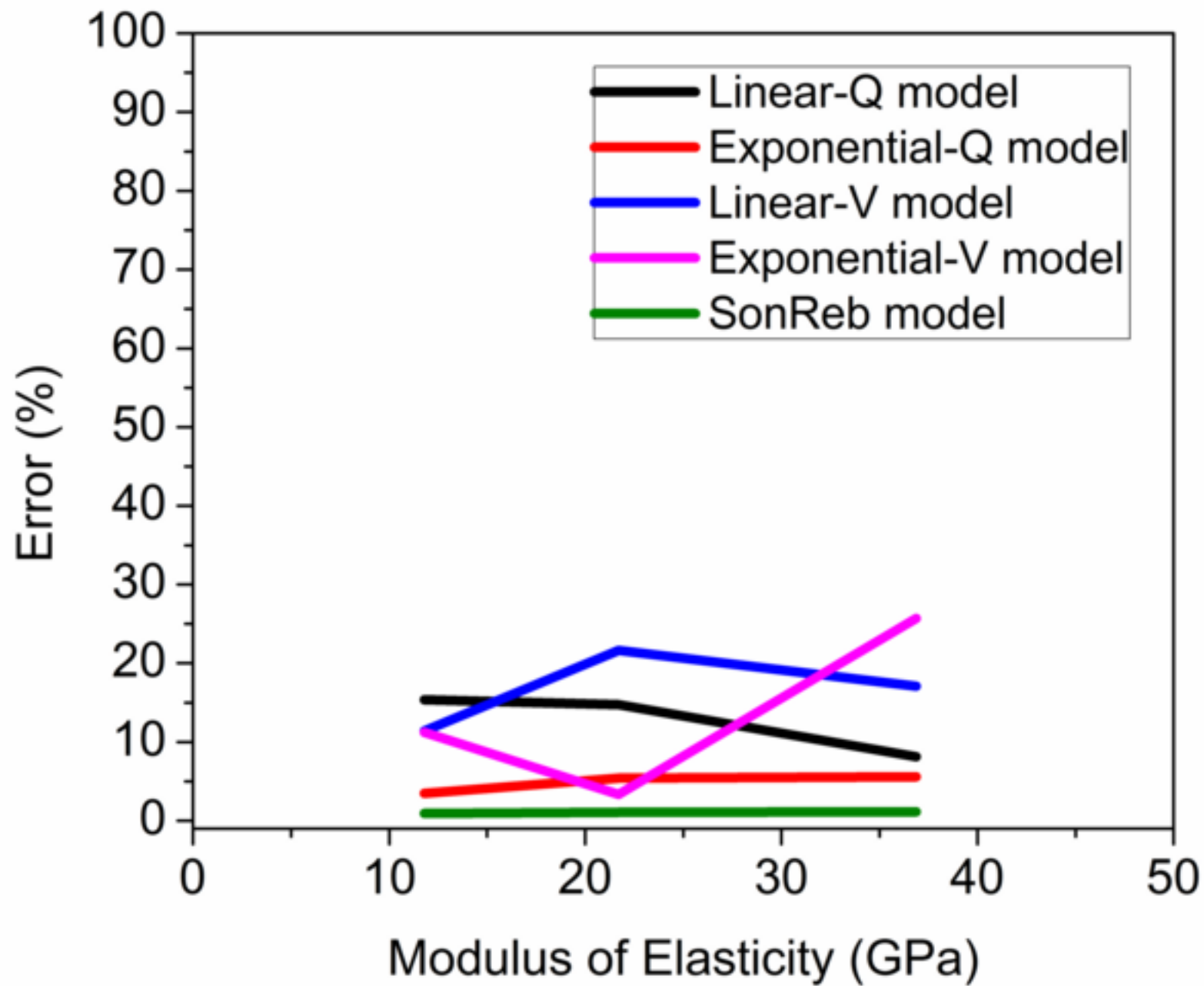


Fig. 17b
[Click here to download high resolution image](#)

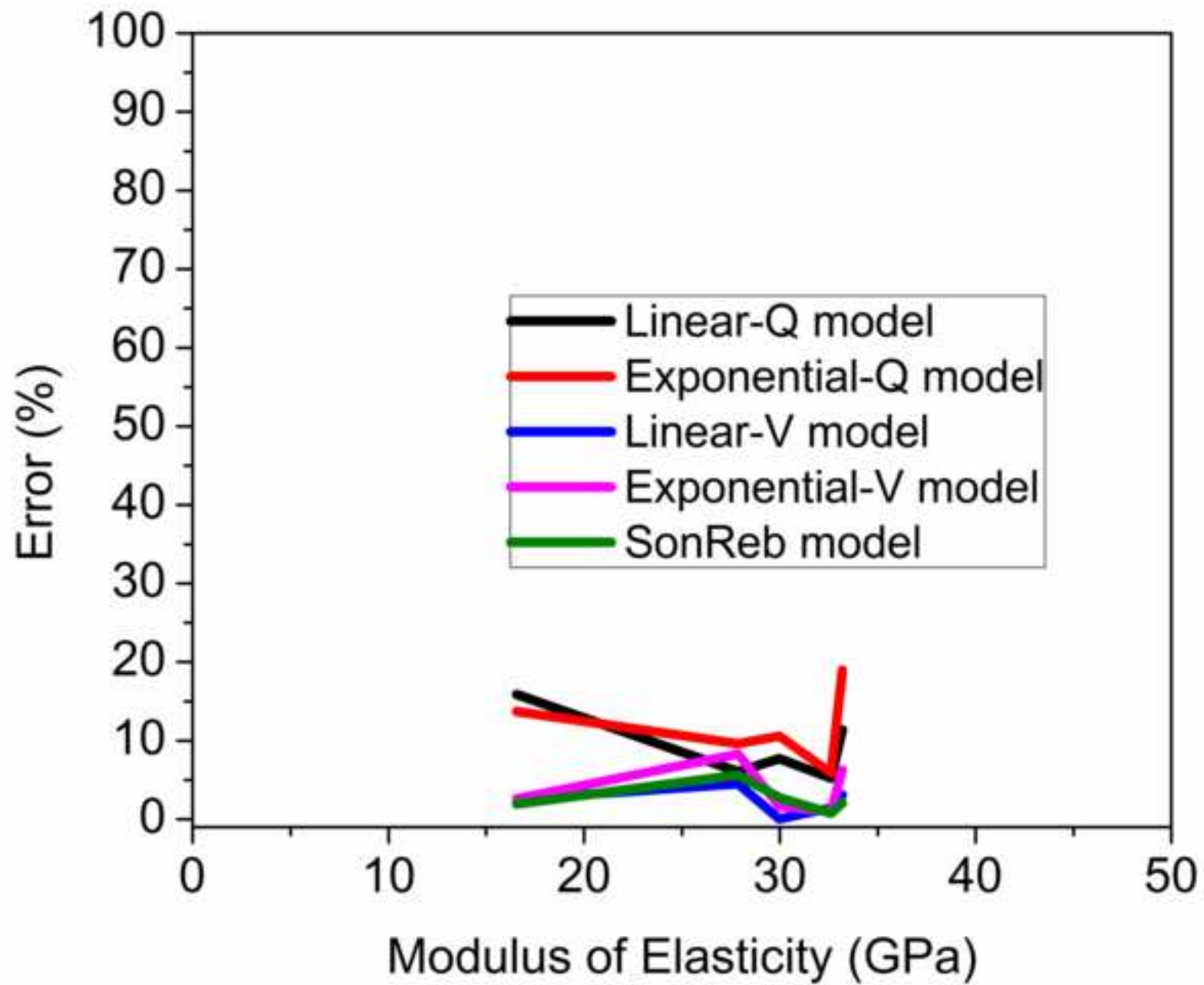


Fig. 17c
[Click here to download high resolution image](#)

